

# Predictive Deployment of UAV Base Stations in Wireless Networks: Machine Learning Meets Contract Theory

Qianqian Zhang<sup>1</sup>, Walid Saad<sup>1</sup>, Mehdi Bennis<sup>2</sup>, Xing Lu<sup>3</sup>, Mérouane Debbah<sup>4,5</sup>,  
and Wangda Zuo<sup>3</sup>

<sup>1</sup>Bradley Department of Electrical and Computer Engineering, Virginia Tech, VA, USA, Emails: {qqz93,walids}@vt.edu

<sup>2</sup>Center for Wireless Communications-CWC, University of Oulu, Finland, Email: mehdi.bennis@oulu.fi

<sup>3</sup>Department of Civil, Environmental and Architectural Engineering, University of Colorado Boulder, CO, USA, Email: {xing.lu-1,wangda.zuo}@colorado.edu

<sup>4</sup>Mathematical and Algorithmic Sciences Lab, Huawei France R&D, Paris, France, Email: merouane.debbah@huawei.com

<sup>5</sup>Large Systems and Networks Group (LANEAS), CentraleSupélec, Université Paris-Saclay, Gif-sur-Yvette, France

## Abstract

In this paper, a novel framework is proposed to enable a predictive deployment of unmanned aerial vehicles (UAVs) as temporary base stations (BSs) to complement ground cellular systems in face of downlink traffic overload. First, a novel learning approach, based on the weighted expectation maximization (WEM) algorithm, is proposed to estimate the user distribution and the downlink traffic demand. Next, to guarantee a truthful information exchange between the BS and UAVs, using the framework of contract theory, an offload contract is developed, and the sufficient and necessary conditions for having a feasible contract are analytically derived. Subsequently, an optimization problem is formulated to deploy an optimal UAV onto the hotspot area in a way that the utility of the overloaded BS is maximized. Simulation results show that the proposed WEM approach yields a prediction error of around 10%. Compared with the expectation maximization and k-mean approaches, the WEM method shows a significant advantage on the prediction accuracy, as the traffic load in the cellular system becomes spatially uneven. Furthermore, compared with a baseline, event-driven allocation, the proposed approach enables UAVs to provide efficient downlink service for hotspot users, and improves the revenues of both the BS and UAV networks significantly.

*Index Terms* – cellular networks; UAV deployment; traffic prediction; contract theory.

## I. INTRODUCTION

The use of unmanned aerial vehicles (UAVs) as flying base stations (BSs) has attracted growing interest in the past few years [1]–[8]. UAV BSs can be deployed to complement the existing cellular systems, by providing reliable wireless services for ground users, to potentially increase

A preliminary version of this work appears in the proceedings of IEEE GLOBECOM 2018 [1].

the network capacity, eliminate coverage holes, and cope with the steep surge of communication needs in hotspot areas [1]. Compared with the terrestrial BSs that are deployed at a fixed location for a long term, UAVs can rapidly change their positions to provide temporary on-demand service [3]. For instance, UAV BSs can be deployed to serve major events (e.g. sport or musical events) during which the terrestrial network capacity is often strained, or to provide communication capabilities for disaster areas in which the ground cellular systems cannot provide regular service [4]. Furthermore, UAVs can adjust their positions and establish line-of-sight (LOS) communication links towards ground users, thus improving network performance [5]. Due to their broad range of application domains and low cost, UAVs as flying BSs is a promising solution to provide temporary connectivity for ground users [6].

However, the UAV deployment for on-demand cellular service faces several key challenges. For instance, UAV BSs are strictly constrained by their on-board energy, which should be efficiently used for communication. However, the on-demand deployment requires UAVs to continuously change their positions to meet instant communication requests. Therefore, most of on-board energy can be consumed by mobility, thus limiting their communication capabilities [1]. Moreover, to effectively alleviate network congestion during a hotspot event, the deployed UAV must have enough on-board power to satisfy the downlink communication demand. In order to find a qualified UAV with sufficient energy, the network operator should estimate the required transmit power, based on the real-time traffic load. These challenges, in turn, motivate the need for a comprehensive prediction of cellular traffic, and a predictive approach for UAV deployment [9]. To this end, machine learning (ML) techniques can be applied to estimate the cellular traffic demand within the target system. Given the predicted traffic load, each BS can detect hotspot areas and request suitable UAVs to alleviate network congestion.

Another challenge of the on-demand deployment for aerial wireless service is to incentivize cooperation between the ground BS and the UAV operators. As shown in [10], the ground BSs and UAVs can belong to different operators who seek to selfishly maximize their individual benefits. Hence, to request a UAV's assistance, a ground BS must offer an appropriate economic reward to the UAV operator for aerial wireless service. However, given that the BS has no prior knowledge of each UAV, there is no guarantee that the requested UAV is able to provide enough transmit power to satisfy the downlink demand. Therefore, designing an incentive mechanism is necessary to ensure a truthful information exchange between the UAV and BS systems.

### A. Related Works

The optimal deployment of UAVs as aerial BSs has recently attracted significant attention [11]–[13]. In [11], the authors studied the optimal locations and coverage areas of aerial BSs under the objective of minimizing the transmit power. The work in [12] derived the minimum number of UAVs to satisfy the coverage and capacity constraints of the wireless system. In [13], the authors jointly optimized the UAV trajectory and the network resource allocation in order to maximize the throughput to ground users. The problem of traffic offloading from an existing wireless network via UAV BSs has been addressed in [14]–[17]. In [14], the allocation problem of UAVs to each geographic area was investigated to improve the spectral efficiency and reduce the delay. In [15] and [16], the authors optimized the trajectory of UAVs to provide wireless services to the cell-edge users. In [17], an unsupervised learning approach was presented to solve the 3D deployment of a fleet of UAVs for traffic offloading. However, most of the existing works [11]–[17] assumed that the traffic demand of the cellular users is known a priori, which is challenging to estimate in a practical network. Furthermore, the works [11]–[17] optimized the performance of the cellular network in a centralized approach which assumes all UAVs belong to the same entity. Given the fact that the UAVs can belong to multiple operators, a new framework is needed to consider the individual utility of UAVs in the aerial communication service, while optimizing the performance of the ground cellular networks.

Meanwhile, in [18]–[20], a number of ML approaches are proposed to predict the data demands of cellular networks. In [18], a traffic prediction framework was proposed to model the cellular data in the temporal and spatial domains. In [19], the authors proposed an ML framework, based on pattern modeling, to predict the locations of mobile users during daily activities. The work [20] provided surveys that focused on the general use of ML algorithms in cellular networks. Furthermore, the prior art in [21]–[23] studied the use of ML techniques to improve the performance of UAV-aided communications. In [21], an ML framework based on liquid state machine is proposed to optimize the caching content of each UAV, as well as the resource allocation strategies. In [22], the authors investigated an ML approach to construct a radio map for autonomous path planning and positioning of UAVs. In [23], ML algorithms are applied to detect and distinguish aerial users from the ground mobile users. However, most of the works in [18]–[23] aim to build an ML model to predict regular traffic patterns, while hotspot events are considered as an anomaly and excluded from these studies. In fact, none of the

approaches proposed in [18]–[23] can effectively identify the hotspot areas or accurately predict excessive traffic load during the hotspot event. Thus, results of these prior works cannot enable a predictive UAV deployment for on-demand cellular service to alleviate the traffic congestion.

### B. Contributions

The main contribution of this paper is a novel framework for optimally deploying UAVs to assist a ground cellular network in alleviating its downlink traffic congestion during hotspot events. The proposed framework divides the deployment process into four, inter-related and sequential stages: learning stage, association stage, movement stage, and service stage. For each stage, we evaluate the performance of the proposed framework, using an open-source dataset in [24]. Our main contributions include:

- A novel framework, based on the weighted expectation maximization (WEM) approach, is proposed to predict the downlink traffic demand for each cellular system in the learning stage. In particular, the proposed approach can identify the user distribution, predict the cellular data demand, and pinpoint the hotspot areas within the cellular system.
- In the association stage, to employ a UAV with sufficient on-board energy to satisfy the downlink demand, the framework of contract theory [25] is introduced, where each overloaded BS can jointly design the transmit power and unit reward of the target UAV. We analytically derive the sufficient and necessary conditions needed to guarantee a truthful information exchange between the BS and UAV operators. Once the association stage is done, each BS will have employed a proper UAV to assist its downlink cellular service.
- Simulation results show that the mean relative error (MRE) of the proposed ML approach is around 10%. Compared with two baselines, an expectation maximization (EM) scheme and a  $k$ -mean algorithm, the proposed method yields a better prediction accuracy, particularly when the downlink traffic load in the cellular system becomes spatially uneven. Furthermore, simulation results show that the designed contract can ensure a non-negative payoff of each employed UAV, and each UAV will truthfully reveal its communication capability by accepting the contract designed for itself.
- We compare the performance of the proposed approach with a baseline, event-driven allocation method, which deploys the closest UAV onto the hotspot area without traffic prediction and contract design. Numerical results show that the proposed predictive method enables UAV operators to provide efficient downlink service for hotspot users, and significantly

improves the economic revenues of both the BS and UAV networks, compared with the event-driven method.

The rest of this paper is organized as follows. In Section II, we present the system model. The problem formulation is given in Section III. In Section IV, the ML approach is proposed to predict downlink traffic demands. In Section V, the feasible contract is designed with the optimal UAV being employed to offload the cellular traffic. Simulation results are presented in Section VI. Finally, conclusions are drawn in Section VII.

## II. SYSTEM MODEL

Consider a set  $\mathcal{I}$  of  $I$  cellular BSs providing downlink wireless service to a group of user equipments (UEs) in a geographical area  $\mathcal{A}$ . Each BS  $i \in \mathcal{I}$  serves an area  $\mathcal{A}_i$ , such that  $\cup_{i \in \mathcal{I}} \mathcal{A}_i = \mathcal{A}$ , and  $\mathcal{A}_i \cap \mathcal{A}_k = \emptyset$  for any  $i \neq k \in \mathcal{I}$ . The spatial distribution of the served UEs for each BS  $i$  is denoted by  $f_i(\mathbf{y})$ , where  $\int_{\mathbf{y} \in \mathcal{A}_i} f_i(\mathbf{y}) d\mathbf{y} = 1$ . A set  $\mathcal{J}$  of  $J$  flying UAVs can provide additional cellular service, if the hotspot events happen in the ground cellular network. We assume that the group BSs and UAVs belong to different network operators, and different frequency bands are used for the ground and aerial downlink transmissions, separately. A single antenna is equipped at each UE that can receive signals from both the ground BS and the UAV. Initially, a UE will connect to one of the ground BSs. However, as shown in Fig. 1, if a ground BS  $i \in \mathcal{I}$  is overloaded in the downlink, BS  $i$  can request the assistant of a UAV to offload the service of some UEs. We assume that a UAV only serves the UEs of a single BS at each time, while each BS can employ multiple UAVs, based on the cellular traffic amount. In this regard, if the downlink traffic demand at the level of a given BS is excessive, such that no single UAV is capable to alleviate communication congestion, then the BS will divide the offloaded UEs into multiple spatially-disjoint sets, and request an individual UAV for each UE set, independently. In order to serve the downlink UEs more efficiently, each UAV is equipped with a directional antenna array that enables beamforming transmissions [26]. As a result, interference between different UAV networks is negligible.

### A. Air-to-ground downlink communications

The path loss of the air-to-ground communication link from a typical UAV located at  $\mathbf{x} \in \mathbb{R}^3$  to a typical ground UE that is located at  $\mathbf{y} \in \mathbb{R}^3$  can be given by [27]:

$$h[dB](\mathbf{x}, \mathbf{y}) = 20 \log \left( \frac{4\pi f_c \|\mathbf{x} - \mathbf{y}\|}{c} \right) + \xi(\mathbf{x}, \mathbf{y}), \quad (1)$$

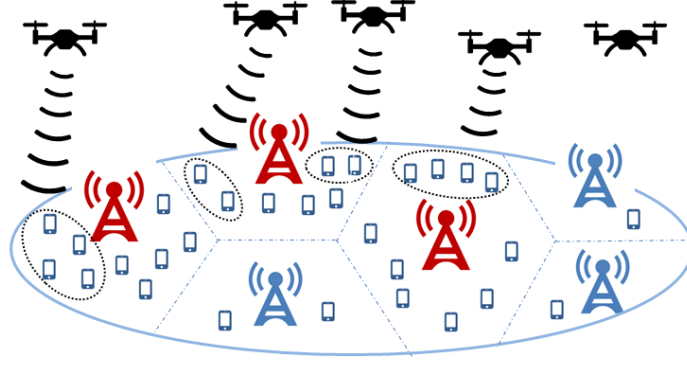


Fig. 1: The red BSs are having excessive traffic load in the downlink, thus each red BS requests a UAV to offload a part of UEs to the aerial cellular system.

where  $f_c$  is the carrier frequency of UAV downlink communications,  $\|\mathbf{x} - \mathbf{y}\|$  is the UAV-UE distance,  $c$  is the speed of light, and  $\xi(\mathbf{x}, \mathbf{y})$  is the additional path loss of the air-to-ground channel, compared with the free space propagation. The value of  $\xi(\mathbf{x}, \mathbf{y})$  can be modeled as a Gaussian distribution with different parameters  $(\mu_{\text{LOS}}, \sigma_{\text{LOS}}^2)$  and  $(\mu_{\text{NLOS}}, \sigma_{\text{NLOS}}^2)$  for the LOS and non-line-of-sight (NLOS) links, respectively. Then, the achievable data rate from a UAV  $j \in \mathcal{J}$  located at  $\mathbf{x}_j$  to a UE located at  $\mathbf{y} \in \mathcal{A}_i$  is

$$r_{ij}(\mathbf{x}_j, \mathbf{y}, p_j) = w \log_2 \left( 1 + \frac{g(\mathbf{x}_j, \mathbf{y}) p_j}{h(\mathbf{x}_j, \mathbf{y}) w n_0} \right), \quad (2)$$

where  $w$  is the downlink bandwidth of each UAV,  $g(\mathbf{x}_j, \mathbf{y})$  is the antenna gain of UAV  $j$  towards the UE located at  $\mathbf{y}$ ,  $p_j$  is the transmit power of UAV  $j$ ,  $h(\mathbf{x}_j, \mathbf{y})$  is the path loss in linear scale, and  $n_0$  is the average noise power spectrum density at the UE. The probability of having a LOS link between UAV  $j$  located at  $\mathbf{x}_j$  and the UE located at  $\mathbf{y}$  is given by [28]:

$$P_{\text{LOS}}(\mathbf{x}_j, \mathbf{y}) = \frac{1}{1 + a \exp(-b[\frac{180}{\pi} \varphi(\mathbf{x}_j, \mathbf{y}) - a])}, \quad (3)$$

where  $a$  and  $b$  are constant values that depend on the communication environment (rural, urban, etc.),  $\varphi(\mathbf{x}_j, \mathbf{y}) = \sin^{-1}(\frac{H_j}{\|\mathbf{x}_j - \mathbf{y}\|})$  is the elevation angle, and  $H_j$  is the altitude of UAV  $j$ . Then, the NLOS probability is  $P_{\text{NLOS}}(\mathbf{x}_j, \mathbf{y}) = 1 - P_{\text{LOS}}(\mathbf{x}_j, \mathbf{y})$ . Consequently, the average downlink rate between a UAV  $j$  and a UE at  $\mathbf{y} \in \mathcal{A}_i$  will be:

$$\bar{r}_{ij}(\mathbf{x}_j, \mathbf{y}, p_j) = P_{\text{LOS}}(\mathbf{x}_j, \mathbf{y}) r_{ij}^{\text{LOS}}(\mathbf{x}_j, \mathbf{y}, p_j) + P_{\text{NLOS}}(\mathbf{x}_j, \mathbf{y}) r_{ij}^{\text{NLOS}}(\mathbf{x}_j, \mathbf{y}, p_j). \quad (4)$$

In order to serve multiple downlink UEs, each UAV applies a time-division-multiple-access (TDMA) technique<sup>1</sup> that divides the time resource evenly among all served UEs, and all bandwidth will be allocated to one single UE during each time slot [29]. By using suitable uplink

<sup>1</sup>The focus of this work is on the deployment stage and, hence, we do not optimize the multiple access scheme type or operation. Optimizing multiple access can be done post-deployment and will be subject to future work.

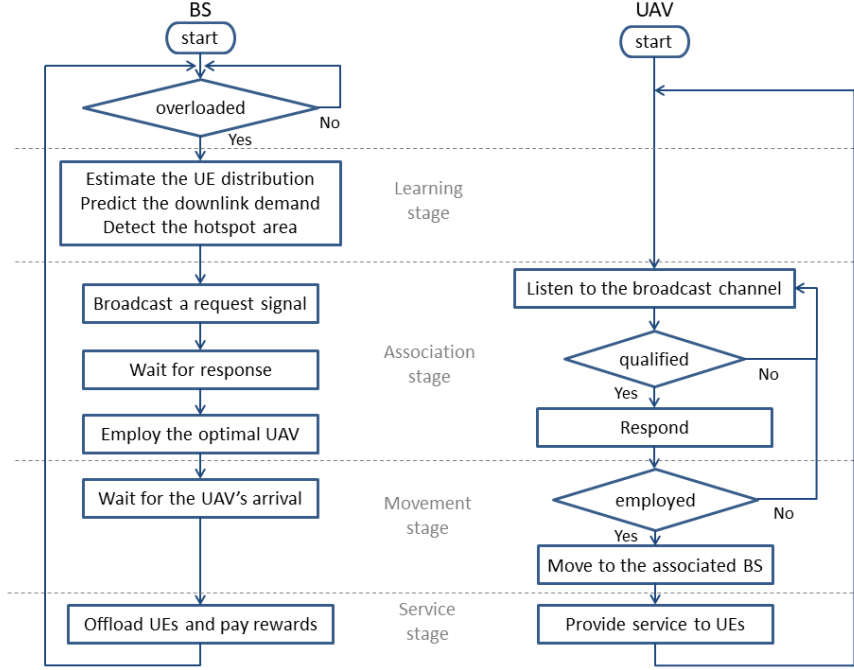


Fig. 2: Flowchart of the proposed UAV predictive deployment process for each BS (left) and each UAV (right).

control signals, the UAV-UE channel can be accurately measured, and thus, the beamforming of UAV's antennas can be properly optimized towards the served UE. Consequently, the average rate that UAV  $j$  can provide to the hotspot UEs from BS  $i$  will be

$$C_{ij}(\mathbf{x}_j, p_j) = \int_{\mathcal{A}_i^c} \bar{r}_{ij}(\mathbf{x}_j, \mathbf{y}, p_j) f_i^c(\mathbf{y}) d\mathbf{y}, \quad (5)$$

where  $\mathcal{A}_i^c \subset \mathcal{A}_i$  is the hotspot area,  $f_i^c(\mathbf{y})$  is the normalized spatial distribution of UEs within  $\mathcal{A}_i^c$ , and  $\int_{\mathcal{A}_i^c} f_i^c(\mathbf{y}) d\mathbf{y} = 1$ . When downlink congestion occurs, BS  $i$  detects the congested area  $\mathcal{A}_i^c$  and offloads the UEs within  $\mathcal{A}_i^c$  to the target UAV.

### B. UAV deployment process

Given the average downlink rate of each UAV in (5), the next step is to deploy suitable UAVs to offload the traffic of a given overloaded BS and, hence, alleviate the downlink congestion of the ground cellular network. To facilitate the analysis, we assume that each UAV serves the associated BS for a constant time interval  $T$ . As shown in Fig. 2, this deployment process can be divided into four sequential stages: learning stage, association stage, movement stage, and service stage. The details of each stage are given as next:

1) *Learning stage:* For each BS  $i \in \mathcal{I}$ , once the downlink communication exceeds its network capacity, a learning stage with a fixed duration  $\tau$  starts. During  $\tau$ , BS  $i$  collects the downlink transmission record  $\mathcal{S}_i = \{(s, \mathbf{y}, t) | \mathbf{y} \in \mathcal{A}_i, t \in [\Delta t, 2\Delta t, \dots, \tau]\}$ , where  $s$  is the downlink data

rate that BS  $i$  provides to the UE located at  $\mathbf{y}$  at time  $t$ , and  $\Delta t$  is the time slot during which the downlink rate can be considered to be constant. Since BS  $i$  does not know the hotspot area  $\mathcal{A}_i^c$  and the UE distribution  $f_i(\mathbf{y})$  when congestion occurs, a learning stage is necessary to estimate the spatial distribution of UEs and the traffic demand of the on-going hotspot event.

Considering common events, such as sport games and outdoor concerts, where mobile users are often confined to seated or geographically constrained spaces, the mobility of hotspot UES is either scarce or very low. Therefore, we assume that the UE distribution  $f_i(\mathbf{y})$  during one  $T$  is time-invariant. Furthermore, to estimate the traffic demand within the congested area, a spatial density function  $S_i(\mathbf{y})$  that evaluates the average data rate per UE is proposed for UE at each location  $\mathbf{y} \in \mathcal{A}_i$ . Consequently, the total data demand  $d_i$  from a hotspot area  $\mathcal{A}_i^c$  during a time interval  $T$  will be given by:

$$d_i = \int_t^{t+T} \int_{\mathbf{y} \in \mathcal{A}_i^c} S_i(\mathbf{y}) d\mathbf{y} dt = T \int_{\mathbf{y} \in \mathcal{A}_i^c} S_i(\mathbf{y}) d\mathbf{y}. \quad (6)$$

The proposed approach for estimating the UE distribution and traffic demand will be discussed in Section IV.

Next, the overloaded BS needs to estimate whether one UAV is sufficient to alleviate its downlink congestion, and to calculate the optimal location of each target UAV. Following from [2, equation (42)] and [11, equations (10) and (11)], given the UE distribution  $f_i^c(\mathbf{y})$  and the hotspot area  $\mathcal{A}_i^c$ , the location  $\mathbf{x}_{ij}^*$  of a target UAV  $j$  in serving BS  $i$  can be derived in a way to minimize the transmit power  $p_{ij}(\mathbf{x}_{ij}^*, \rho_i^c)$ , while satisfying the average rate requirement  $\rho_i^c$  per UE. The average rate per UE is defined by the ratio of the sum data rate within the hotspot area  $\mathcal{A}_i^c$  over the total number of hotspot UEs  $Q_i^c$ , thus  $\rho_i^c = \frac{d_i}{TQ_i^c}$ . Therefore, the optimal service location of the target UAV can be calculated by BS  $i$ , prior to the UAV's deployment. We define  $p_{\max}$  to be the maximum transmit power of each UAV, which is limited by the antennas' hardware. Then, once  $d_i > TC_{ij}(\mathbf{x}_{ij}^*, p_{\max})$ , any UAV  $j \in \mathcal{J}$  will no longer be sufficient to satisfy the downlink demand  $d_i$ . In this case, BS  $i$  will divide the offloaded UEs evenly into  $N$  disjoint subsets, where  $N$  is the minimal integer to guarantee that, for each subset  $n = 1, \dots, N$ , the following requirement holds:

$$d_i(n) = \frac{d_i}{N} < TC_{ij}(\mathbf{x}_{ij}^*(n), p_{\max}). \quad (7)$$

Next, BS  $i$  will request a UAV for each UE subset, independently.



2) *Association stage* : In the association stage, each overloaded BS  $i$  requests the assistance of a UAV, by broadcasting a signal with the downlink demand  $d_i(n)$  and the service location  $\mathbf{x}_{ij}^*(n)$  for each UE subset  $n$ . A first-call-first-serve scheme is applied, and each BS  $i \in \mathcal{I}$  will listen to the broadcast channel before sending the signal. If the channel is occupied by another BS, then BS  $i$  will wait until the on-going association is completed. For each BS  $i$ , the goal is to request a UAV that has enough on-board power to meet the downlink demand  $d_i$  of UEs within  $\mathcal{A}_i^c$ . The optimal UAV association to each overloaded BS will be studied in Section V.

3) *Movement stage*: After the association stage, the selected UAV  $j$  starts to move from its current location  $\mathbf{x}_j$  to the service point  $\mathbf{x}_{ij}^*$  of its target BS  $i$ . The duration  $t_{ij}$  of the movement stage depends on the distance  $\|\mathbf{x}_j - \mathbf{x}_{ij}^*\|$  and the average speed  $v_j$  of UAV  $j$ .

4) *Service stage*: Once it reaches the service point, UAV  $j$  will provide downlink communications to its group of associated UEs for a time period  $T - t_{ij}$ . Note that, during the movement and service stages, the employed UAV is fully dedicated to its associated BS. Thus, the UAV cannot be requested by any other BSs until the end of its current service. Furthermore, to guarantee a sufficient service time, the maximum travel time of UAV  $j$  is limited by  $t_{ij} \leq \kappa_i T$ , where  $\kappa_i \in (0, 1)$ . If the travel time exceeds  $\kappa_i T$ , UAV  $j$  is not a potential choice for BS  $i$ .

Here, in order to optimally associate a UAV to each overloaded ground BS, we first define a utility function that each BS aims to maximize when selecting a UAV to offload cellular traffic in Section II-C. Meanwhile, the UAV's utility function is given in Section II-D that defines an economic payoff of each UAV from serving an overloaded BS.

### C. Utility function of a ground BS

In the considered network, by using TDMA, the employed UAV  $j$  will evenly divide the service time  $T - t_{ij}$  to all downlink UEs within  $\mathcal{A}_i^c$ . Considering the signal overhead and channel measurement process, we assume the total efficient transmission time is  $\eta(T - t_{ij})$ , where  $\eta \in (0, 1)$ . Therefore, based on the average downlink rate in (5), the achievable data amount that UAV  $j$  can provide to the UEs of BS  $i$  is

$$B_{ij}(p_j) = \eta(T - t_{ij})C_{ij}(p_j). \quad (8)$$

Note that, the movement duration  $t_{ij}$  and the transmit power  $p_j$  are private information for UAV  $j$ , and, thus, BS  $i$  cannot know their values during the service request process. Then, the utility

of BS  $i$ , by employing UAV  $j$  to offload the excess cellular traffic, will be:

$$U_{ij}(u_i, p_j, d_i) = \beta B_{ij}(p_j) - u_i d_i, \quad (9)$$

where  $\beta$  is the payment from each UE to BS  $i$  (per bit of downlink data service), and  $u_i$  is the unit payment that BS  $i$  gives to UAV  $j$  (per bit of aerial data transmission). Thus, the first term in (9) represents the reward that BS  $i$  gets from its UEs by employing UAV  $j$  to provide aerial cellular service, and the second term is the total payment that BS  $i$  gives to UAV  $j$ , based on the estimated downlink demand  $d_i$ .

#### D. Energy model and utility function of a UAV

In the considered problem, the power consumption of each UAV consists of three main components: the aforementioned transmit power  $p_j$ , the propulsion power  $m$ , and the hovering power  $p_h$ . For tractability and as done in [30], we ignore the acceleration and deceleration stages during the UAV's movement, and consider the propulsion power  $m$  to be constant, given an average flying speed. Then, the travel time  $t_{ij}$  can be uniquely determined based on the moving distance  $\|\mathbf{x}_j - \mathbf{x}_{ij}^*\|$ . For each UAV  $j$ , let  $E_j$  be its available on-board energy before the movement stage. Then, during the service stage, the maximum available power that UAV  $j$  can use for downlink transmissions will be  $p_{ij}^{\max} = \frac{E_j - mt_{ij} - p_h(T - t_{ij})}{T - t_{ij}}$ , where  $mt_{ij}$  is the energy consumed during the UAV's movement, and  $p_h(T - t_{ij})$  is the hovering energy during the service stage. Therefore, the transmit power  $p_j$  will fall within  $[p_{ij}(\mathbf{x}_{ij}^*, \rho_i^c), \min\{p_{ij}^{\max}, p_{\max}\}]$ , where  $p_{ij}(\mathbf{x}_{ij}^*, \rho_i^c)$  is the minimum required power to satisfy the downlink data demand, and  $p_{\max}$  is the maximum transmit power. Without loss of generality, we assume that  $p_{ij}(\mathbf{x}_{ij}^*, \rho_i^c) \leq \min\{p_{ij}^{\max}, p_{\max}\}$  holds. Otherwise, UAV  $j$  is not a potential option for BS  $i$ . Consequently, the utility that a UAV  $j \in \mathcal{J}$  can achieve from providing the aerial cellular service to the UEs of BS  $i$  will be:

$$R_{ij}(u_i, p_j, d_i) = u_i d_i - \alpha[p_j(T - t_{ij}) + p_h(T - t_{ij}) + mt_{ij}], \quad (10)$$

where  $\alpha$  is a unit cost per Joule of UAV's on-board energy. The first term in (10) is the reward that UAV  $j$  obtains from serving BS  $i$ , and the second term in (10) is the energy cost, where  $p_j(T - t_{ij})$  is the energy for downlink transmissions. Note that, the data demand  $d_i$  is estimated by BS  $i$  during the learning stage. Therefore, during the association stage,  $d_i$  in (9) and (10) is considered as a constant. Moreover, the unit payment  $u_i$  and the transmit power  $p_j$  are the variables, controlled by BS  $i$  and UAV  $j$ , respectively.

### III. PROBLEM FORMULATION

The objective of a BS in face of downlink congestion is to employ a suitable UAV with sufficient on-board power to offload excessive cellular traffic, while maximizing the utility function in (9). Meanwhile, the goal of each UAV is to serve an overloaded BS, such that its utility in (10) can be optimized. However, by comparing (9) and (10), we realize that  $\arg \max_{u_i, p_j} U_{ij} = \arg \min_{u_i, p_j} R_{ij}$  and  $\arg \max_{u_i, p_j} R_{ij} = \arg \min_{u_i, p_j} U_{ij}$ . Therefore, each BS-UAV pair has conflicting interests. Given that the BSs and UAVs belong to different operators, each will maximize its own utility. The conflict between each BS and each UAV is irreconcilable.

Meanwhile, we note that the values of the unit payment  $u_i$  and the data demand  $d_i$  will be broadcast by BS  $i$  during the association stage. Thus, each UAV  $j$  has all necessary information to determine its utility. However, BS  $i$  cannot easily acquire some of the private information of each UAV  $j$ , such as its current location and available onboard energy. Such information determines the travel time of each UAV to the service point, and the downlink communication capacity of each UAV BS, and, thus, it is essential for the BS to have accurate information in order to evaluate the performance of each UAV's service. However, each UAV may have an incentive to misrepresent its location or energy in order to obtain a higher utility. For example, by misrepresenting its location as being closer to the requesting BS than it actually is, a UAV gets a higher priority from the BS, due to a misperceived shorter waiting time. Such a misleading behavior will harm the utility of each overloaded BS. Therefore, it is necessary to design a mechanism to guarantee a truthful information exchange between the BS and UAVs. To this end, each BS  $i$  can jointly design  $(u_i, p_j)$  to ensure that their values are beneficial for both the BS and UAV operators, so that the conflict of interest can be properly resolved between the BS and the UAV group. Therefore, we let  $\phi_{ij} = (u_i, p_j)$  be a *traffic offload contract*, which captures the values of  $p_j$  and  $u_i$  if BS  $i$  employs UAV  $j$  to offload its hotspot UEs. In order to understand the relationship between the unit payment  $u_i$  and the transmit power  $p_j$ , we divide both sides of (10) by  $\alpha(T - t_{ij})$  and rewrite the utility of UAV  $j$  as follows:

$$\begin{aligned} \tilde{R}_{ij}(u_i, p_j, d_i) &= \frac{d_i}{\alpha(T - t_{ij})} u_i - p_j - \frac{mt_{ij}}{T - t_{ij}} - p_h, \\ &= \theta_{ij} u_i - p_j - M_{ij}, \end{aligned} \tag{11}$$

where the values of  $\theta_{ij} = \frac{d_i}{\alpha(T - t_{ij})}$  and  $M_{ij} = \frac{mt_{ij}}{T - t_{ij}} + p_h$  are determined for each BS-UAV pair.

Since  $\theta_{ij}$  determines the sensitivity of  $\tilde{R}_{ij}$  to the increase of  $u_i$  and  $p_j$  in (11), its value is essential for the joint design of  $(u_i, p_j)$ . Therefore, we define  $\theta_{ij}$  as the *type* of UAV  $j$  with

respect to BS  $i$ , and the range of  $\theta_{ij}$  is denoted by  $\Theta = [\theta^{\min}, \theta^{\max}]$ , with  $\theta^{\min} > 0$ . However, due to the privacy of  $t_{ij}$ , the type  $\theta_{ij}$  of each UAV  $j \in \mathcal{J}$  is unknown for BS  $i$ . In order to design the contract without knowing each UAV's type, before broadcasting the request signal, BS  $i$  will design a set of contracts  $\Phi_i(\Theta) = \{\phi_{ij}(\theta_{ij}) | \forall \theta_{ij}\} = \{(u_i(\theta_{ij}), p_j(\theta_{ij})) | \forall \theta_{ij}\}$  for all UAV types  $\theta_{ij} \in \Theta$ , where  $u_i(\theta_{ij})$  represents the payment that BS  $i$  pays to UAV  $j$  per bit of data, given that UAV  $j$  is of type  $\theta_{ij}$ , and  $p_j(\theta_{ij})$  is the transmit power that UAV  $j$  of type  $\theta_{ij}$  provides to serve BS  $i$ . Then, (11) becomes  $\tilde{R}(\theta_{ij}) = \theta_{ij}u_i(\theta_{ij}) - p_j(\theta_{ij}) - M_{ij}$ .

Meanwhile, to ensure that the employed UAV will accept the contract of its own type and provide enough transmit power to meet the downlink demand, two constraints, based on contract theory [25], must be considered, which are individual rationality (IR) condition and incentive compatibility (IC) condition, defined as follows.

**Definition 1** (Individual Rationality). *A contract designed by BS  $i$  satisfies the IR constraint, if a UAV of any type  $\theta_{ij} \in \Theta$  will receive a non-negative payoff from BS  $i$  by accepting the contract item for type  $\theta_{ij}$ , i.e.  $\theta_{ij}u_i(\theta_{ij}) - p_j(\theta_{ij}) - M_{ij} \geq 0, \forall \theta_{ij} \in \Theta$ .*

A contract satisfying the IR condition guarantees that the reward that each UAV  $j \in \mathcal{J}$  can obtain from serving BS  $i$  is great than or equal to zero. Compared with the non-employed state in which the payoff is always zero, each UAV is willing to accept the contract from the requesting BS, as long as its contract satisfies the IR condition.

**Definition 2** (Incentive Compatibility). *A contract designed by BS  $i$  satisfies the IC constraint, if a UAV of type  $\theta_{ij}$  will get the highest utility from BS  $i$  by accepting the contract designed for its own type  $\theta_{ij}$ , compared with all the other types  $\theta$  in  $\Theta$ , i.e.  $\theta_{ij}u_i(\theta_{ij}) - p_j(\theta_{ij}) - M_{ij} \geq \theta_{ij}u_i(\theta) - p_j(\theta) - M_{ij}, \forall \theta \in \Theta$ .*

A contract satisfying IC condition guarantees that each UAV  $j$  will only accept the contract designed for its own type  $\theta_{ij}$ , since accepting the contract of any other type  $\theta \in \Theta$  will result in a lower or the same reward. A contract satisfying both IR and IC conditions is called a *feasible* contract, which ensures the UAV will accept and only accept the contract designed for its type.

Consequently, for each BS  $i \in \mathcal{I}$  in face of downlink traffic congestion, the objective is to maximize its utility in (9), by estimating the downlink data demand  $d_i$  within the hotspot area  $\mathcal{A}_i^c$ , designing the contract set  $\Phi_i$  for each UAV of any type in  $\Theta$ , and determining an optimal UAV  $j \in \mathcal{J}$  to offload the excessive cellular service. We formulate this predictive UAV deployment

problem as follows,

$$\max_{\{(u_i(\theta_{ij}), p_j(\theta_{ij})) | \forall \theta_{ij}\}, j \in \mathcal{J}} U_{ij}(u_i(\theta_{ij}), p_j(\theta_{ij}), d_i), \quad (12a)$$

$$\text{s. t. } R_{ij}(\theta_{ij}) \geq 0, \quad (12b)$$

$$R_{ij}(\theta_{ij}) \geq R_{ij}(\theta), \forall \theta \in \Theta, \quad (12c)$$

$$p_{ij}(\mathbf{x}_{ij}^*, \rho_i^c) \leq p_j(\theta_{ij}) \leq \min\{p_{ij}^{\max}, p_{\max}\}, \quad (12d)$$

$$t_{ij} \leq \kappa_i T, \quad (12e)$$

$$d_i > 0, u_i(\theta_{ij}) > 0. \quad (12f)$$

The objective function (12a) is the utility that BS  $i$  obtains from employing UAV  $j$  of type  $\theta_{ij}$ . (12b) and (12c) are the IR and IC constraints, respectively. (12d) is the constraint on the transmit power, and (12e) limits the maximum travel time. (12f) imposes a positive downlink demand within  $\mathcal{A}_i^c$ , and a positive unit payment. Note that, the IC constraint (12c) is an optimization problem, which must be first addressed in order to guarantee that each UAV receives the highest payoff by accepting the contract item of its own type. Meanwhile, given any  $\theta_{ij} \in \Theta$ , the objective function and all constraints in (12) are jointly determined. Thus, the variable  $\theta_{ij}$  becomes the key to finding the optimal association result. In order to simplify the optimization problem (12), we can derive the necessary and sufficient conditions for IC and IR constraints, based on the UAV type  $\theta_{ij}$ , which essentially reduces to the problem of designing a feasible contract.

Consequently, in order to solve the predictive UAV deployment problem in (12), first, a learning-based approach is proposed for each BS  $i \in \mathcal{I}$  to predict the downlink demand  $d_i$  of the offloaded UEs in Section IV. Next, the feasible traffic offload contract  $\Phi_i$  is developed in Section V, with the optimal UAV being selected to maximize the utility of the requesting BS  $i$ .

#### IV. LEARNING STAGE: ESTIMATION OF CELLULAR TRAFFIC DEMAND

In this section, our goal is to estimate the UE distribution and the downlink data demand during a hotspot event of an overloaded BS. This estimation is necessary to solve (12) because the downlink data demand  $d_i$  is considered as a known value in the association stage, which determines the type  $\theta_{ij}$  of each UAV  $j$  with respect to the overloaded BS  $i$ . To enable an accurate modeling, each BS  $i$  collects the downlink transmission records  $\mathcal{S}_i$  during the learning stage. For notation simplicity, let  $N$  be the total number of records in  $\mathcal{S}_i$ . Then, the downlink transmission dataset  $\mathcal{S}_i$  can be rewritten as  $\{(s_n, \mathbf{y}_n, t_n) | n = 1, \dots, N\}$ . Given the aggregated locations of the

UEs within the hotspot area, the user distribution and the downlink traffic demand are assumed to be time-invariant during  $T$ . Based on  $\mathcal{S}_i$ , we extract the spatial distribution  $f_i(\mathbf{y})$  of the downlink UEs in Section IV-A, and then, in Section IV-B the downlink data rate  $S_i(\mathbf{y})$  is modeled, and the hotspot area  $\mathcal{A}_i^c$  is determined, sequentially. Once this is done, the average rate of each UAV can be given by (5), and the downlink data demand  $d_i$  will be found from (6).

#### A. Estimation of the UE distribution

Given the downlink transmission record  $\mathcal{S}_i$ , BS  $i$  can model the UE distribution, using the location information  $\mathcal{Y} = \{\mathbf{y}_1, \dots, \mathbf{y}_N\}$ , where each data point  $\mathbf{y}_n \in \mathcal{Y}$  indicates the existence of a downlink UE. We assume that the UEs' locations follow a latent distribution  $f_i(\mathbf{y})$ , and each record  $\mathbf{y}_n$  is an independent sample from this distribution. A Gaussian mixture model (GMM), which is the weighted sum of multiple Gaussian distributions, can model the distribution of downlink UEs, as follows:

$$f_i(\mathbf{y}) = \sum_{l=1}^L \omega_l \mathcal{N}(\mathbf{y} | \boldsymbol{\mu}_l, \boldsymbol{\Sigma}_l), \quad (13)$$

where  $L$  is the number of Gaussian distributions,  $\omega_l \in (0, 1)$  is the weight of the  $l$ -th Gaussian with  $\sum_l \omega_l = 1$ , and  $\boldsymbol{\mu}_l, \boldsymbol{\Sigma}_l$  are the mean and the variance of the  $l$ -th Gaussian. The value of  $\omega_l$  represents the probability that the data point  $\mathbf{y}$  is generated by the  $l$ -th distribution. GMM has been widely applied in [31]–[33] to model the distribution of a latent variable based the sampled data. In particular, due to its special feature of multiple clusters, GMM is a appropriate model of the UE distribution in the congested cellular network, where each hotspot area with a excessive UE density corresponds to a Gaussian center in the GMM.

Given the sampled location record  $\mathcal{Y}$ , the expectation-maximization (EM) algorithm [33] can be applied to optimize the parameters  $\{\omega_l, \boldsymbol{\mu}_l, \boldsymbol{\Sigma}_l\}_{l=1, \dots, L}$  in (13) via an iterative approach, which maximizes the following log of the likelihood function:

$$\ln p(\mathcal{Y} | \boldsymbol{\omega}, \boldsymbol{\mu}, \boldsymbol{\Sigma}) = \ln \Pi_{n=1}^N \left( \sum_{l=1}^L \omega_l \mathcal{N}(\mathbf{y}_n | \boldsymbol{\mu}_l, \boldsymbol{\Sigma}_l) \right). \quad (14)$$

After initialization, the EM algorithm alternates between the E and M steps. In the E step, the posterior probability that  $\mathbf{y}_n$  is generated by the  $l$ -th Gaussian is calculated by

$$v_{nl} = \frac{\omega_l \mathcal{N}(\mathbf{y}_n | \boldsymbol{\mu}_l, \boldsymbol{\Sigma}_l)}{\sum_{z=1}^L \omega_z \mathcal{N}(\mathbf{y}_n | \boldsymbol{\mu}_z, \boldsymbol{\Sigma}_z)}. \quad (15)$$

Then, in the M step, the parameters are updated using the posterior probability (15) by

$$\boldsymbol{\mu}_l = \frac{\sum_n v_{nl} \mathbf{y}_n}{\sum_n v_{nl}}, \quad \boldsymbol{\Sigma}_l = \frac{\sum_n v_{nl} (\mathbf{y}_n - \boldsymbol{\mu}_l)(\mathbf{y}_n - \boldsymbol{\mu}_l)^T}{\sum_n v_{nl}}, \quad \omega_l = \frac{\sum_n v_{nl}}{N}. \quad (16)$$

After each EM iteration, the updated parameters will result in an increase of the log likelihood function in (14), and the algorithm is guaranteed to converge to a local optimum [33].

### B. Estimation of the downlink data rate

In order to predict the downlink demand  $d_i$ , the spatial feature of the cellular traffic needs to be properly captured by each overloaded BS  $i$ , based on the real-time transmission  $\mathcal{S}_i$ . Given the assumption that the data demand is time-invariant during  $T$ , the temporal variance in  $\mathcal{S}_i$  can be eliminated by averaging the downlink rate at each location over the learning duration  $\tau$ . Thus, we define the *density* of the downlink data rate at location  $\mathbf{y} \in \mathcal{A}_i$  as

$$\bar{S}_i(\mathbf{y}) = \frac{\sum_{(s_n, \mathbf{y}, t_n) \in \mathcal{S}_i} s_n \Delta t}{\tau}, \quad (17)$$

which is the average rate from BS  $i$  towards UEs located at  $\mathbf{y}$  during the learning stage  $\tau$ . To generalize the traffic density  $\bar{S}_i(\mathbf{y})$  into a continuous model that captures the spatial features of the UEs' downlink demand, a Gaussian mixture function (GMF) is proposed as follow,

$$S_i(\mathbf{y}) = \sum_{k=1}^K \pi_k \exp \left( \frac{-(\mathbf{y} - \boldsymbol{\mu}_k)^T \boldsymbol{\Sigma}_k^{-1} (\mathbf{y} - \boldsymbol{\mu}_k)}{2} \right), \quad (18)$$

where  $K$  is the number of basis functions,  $\pi_k$  is the linear coefficient, and  $\boldsymbol{\mu}_k \in \mathcal{A}_i$  and  $\boldsymbol{\Sigma}_k$  are the mean and variance of the  $k$ -th Gaussian function in the GMF. Therefore, the traffic density at location  $\mathbf{y}$  is modeled by the sum of  $K$  Gaussian functions with coefficient  $\{\pi_k\}_{k=1, \dots, K}$ .

However, it should be noted that GMF in (18) is different from GMM in (13) for two reasons. First, a GMF does not have a probabilistic interpretation. In particular, (18) is a deterministic function that calculates the traffic density at each location  $\mathbf{y}$  by adding the values of  $K$  Gaussian function with different linear coefficients. Second, different from the weight in GMM where  $\omega_l \in (0, 1)$  and  $\sum_l \omega_l = 1$ , the value of each linear coefficient  $\pi_k$  is usually much greater than one, and there is no constraint on  $\sum_{k=1}^K \pi_k$ . On the other hand, although (18) has a similar expression to the traditional linear regression model, a significant difference is that GMF has the undetermined parameters  $\pi_k$ ,  $\boldsymbol{\mu}_k$  and  $\boldsymbol{\Sigma}_k$  of each Gaussian function in (18). Thus, existing algorithms for the linear regression with fixed basis functions are not applicable in this problem.

In order to properly model the downlink traffic density  $\bar{S}_i$ , the parameters  $\{\pi_k, \boldsymbol{\mu}_k, \boldsymbol{\Sigma}_k\}_{k=1, \dots, K}$  in (18) need to be optimized. Here, the EM method is not suitable to the traffic density modeling

for two reasons. First, given that each data point  $\mathbf{y}_n$  has a different traffic density  $\bar{S}_i(\mathbf{y}_n)$ , the weight of each location  $\mathbf{y}_n$  in determining the parameter values of  $\boldsymbol{\mu}_k$  and  $\boldsymbol{\Sigma}_k$  should be different to capture the spatial diversity of the traffic load within the cellular network. Meanwhile, given that the downlink traffic density  $S_i(\mathbf{y})$  at each location  $\mathbf{y}$  is usually greater than one, the weight  $\pi_k$  for each  $k$  should not be normalized as is the case in the EM method, and different traffic load at each location should be considered in determining the value of  $\pi_k$ . Therefore, by adding the weight  $\bar{S}_i(\mathbf{y}_n)$  to each data point  $\mathbf{y}_n$ , a weighted expectation maximization (WEM) algorithm is proposed to find the parameters of the traffic density model  $S_i(\mathbf{y})$  in (18).

In the proposed WEM method, the initial value of each Gaussian center  $\boldsymbol{\mu}_k$  is the location  $\mathbf{y}_k$  that has the  $k$ -th highest traffic density in  $\bar{S}_i(\mathbf{y})$ , where  $\mathbf{y} \in \{\mathbf{y}_1, \dots, \mathbf{y}_N\}$ . The initial variance  $\boldsymbol{\Sigma}_k$  equals the identity matrix, and the weight  $\pi_k = \frac{1}{K} \sum_{\mathbf{y}} \bar{S}_i(\mathbf{y})$ . Then, the WEM algorithm updates the values of  $\{\pi_k, \boldsymbol{\mu}_k, \boldsymbol{\Sigma}_k\}_{k=1, \dots, K}$  via an iterative approach. In the E step, the percentage that each Gaussian function  $k$  contributes to the value of the traffic density at location  $\mathbf{y}_n$  is evaluated via  $v_{nk} = \frac{\pi_k \mathcal{N}(\mathbf{y}_n | \boldsymbol{\mu}_k, \boldsymbol{\Sigma}_k)}{\sum_{k=1}^K \pi_k \mathcal{N}(\mathbf{y}_n | \boldsymbol{\mu}_k, \boldsymbol{\Sigma}_k)}$ , which is the same as the traditional EM method in (15). However, in the M step of WEM method, the parameters of each Gaussian function will be updated in a weighted approach, where the mean  $\boldsymbol{\mu}_k$  is recalculated via

$$\boldsymbol{\mu}_k = \frac{\sum_n v_{nk} \mathbf{y}_n \bar{S}_i(\mathbf{y}_n)}{\sum_n v_{nk} \bar{S}_i(\mathbf{y}_n)}, \quad (19)$$

which is a sum of all locations  $\mathbf{y}_n \in \mathcal{Y}$ , weighted by both the posterior probability  $v_{nk}$  and the traffic density  $\bar{S}_i(\mathbf{y}_n)$ . Therefore, the location  $\mathbf{y}_n$  with a higher traffic density  $\bar{S}_i(\mathbf{y}_n)$  will have a higher weight in determining the value of  $\boldsymbol{\mu}_k$ , and the center of Gaussian  $k$  will gradually be driven closer to the high-density locations. Similarly, the variance  $\boldsymbol{\Sigma}_k$  and the linear coefficient  $\pi_k$  of each Gaussian function is also updated, with weights  $\bar{S}_i(\mathbf{y}_n)$ , by

$$\boldsymbol{\Sigma}_k = \frac{\sum_n v_{nk} (\mathbf{y}_n - \boldsymbol{\mu}_k)(\mathbf{y}_n - \boldsymbol{\mu}_k)^T \bar{S}_i(\mathbf{y}_n)}{\sum_n v_{nk} \bar{S}_i(\mathbf{y}_n)}, \quad \pi_k = \frac{\sum_n v_{nk} \bar{S}_i(\mathbf{y}_n)}{\sum_k \sum_n v_{nk} \bar{S}_i(\mathbf{y}_n)}. \quad (20)$$

Furthermore, similar to the EM approach, a WEM method will converge to a local optimum, which maximizes the weighted conditional log-likelihood function [1].

The hotspot area  $\mathcal{A}_i^c$  is a location set in which the traffic density is much higher than other locations in  $\mathcal{A}_i$ . Given the traffic density model  $S_i$ , the average traffic density in  $\mathcal{A}_i$  is calculated via  $\bar{s}_i = \frac{1}{|\mathcal{A}_i|} \int_{\mathbf{y} \in \mathcal{A}_i} S_i(\mathbf{y}) d\mathbf{y}$ , where  $|\mathcal{A}_i|$  denotes the area of  $\mathcal{A}_i$ . Then, the potential hotspot areas are selected to be the neighborhoods near the center  $\{\boldsymbol{\mu}_k\}_{k=1, \dots, K}$  of each Gaussian. Next, by calculating the traffic density at each center, the mean  $\boldsymbol{\mu}_k^*$  with the highest traffic density is



chosen to be the hotspot center, and its neighborhood area, where the traffic density is higher than  $\bar{s}_i$  forms the hotspot area  $\mathcal{A}_i^c$ . The downlink UEs within  $\mathcal{A}_i^c$  will be offloaded to the aerial cellular network. Based on the traffic density model  $S_i(\mathbf{y})$  and the hotspot area  $\mathcal{A}_i^c$ , the predicted data amount  $d_i$  for a time interval  $T$  can be calculated based on (6).

Given the downlink traffic demand  $d_i$  and the UE distribution  $f_i(\mathbf{y})$ , all variables in (12) have determined values, except for the unit payment  $u_i$  and the transmit power  $p_j$ . The next step to solve (12) is to jointly decide the value of  $(u_i, p_j)$ , by designing the feasible contract between an overloaded BS  $i$  with each UAV  $j \in \mathcal{J}$ .

## V. ASSOCIATION STAGE: CONTRACT DESIGN AND UAV ALLOCATION

### A. Contract design

Given the predicted traffic demand  $d_i$ , a BS  $i \in \mathcal{I}$  can request a UAV and offload the UEs within the hotspot area  $\mathcal{A}_i^c$ , so that the future downlink congestion can be alleviated. However, to employ a qualified UAV to meet the downlink demand, each BS needs to carefully design the contract  $\Phi_i = \{(u_i(\theta_{ij}), p_j(\theta_{ij})) | \forall \theta_{ij} \in \Theta\}$  for UAVs of any type  $\theta_{ij}$ . The feasible contract satisfying the IR and IC conditions can guarantee that each UAV  $j \in \mathcal{J}$  will accept the contract designed for its own type and provide the required transmit power to serve the downlink UEs. Thus, to develop a feasible contract set for the requesting BS, we first analyze the sufficient and necessary conditions for a contract to satisfy IC and IR constraints.

**Proposition 1.** *[Necessary Condition] For any  $\theta_{ij}, \theta'_{ij} \in \Theta$ , if  $\theta_{ij} > \theta'_{ij}$ , then  $u_i(\theta_{ij}) \geq u_i(\theta'_{ij})$  and  $p_j(\theta_{ij}) \geq p_j(\theta'_{ij})$ .*

*Proof.* See Appendix A. □

Proposition 1 shows that for a typical UAV  $j$  in  $\mathcal{J}$ , if its type with respect to a typical BS  $i$  increases from  $\theta'_{ij}$  to  $\theta_{ij}$ , then it will receive a higher unit payment  $u_i(\theta_{ij}) \geq u_i(\theta'_{ij})$  from BS  $i$ , and in return, it should provide a larger transmit power  $p_j(\theta_{ij}) \geq p_j(\theta'_{ij})$  in its downlink transmission. Given the definition of  $\theta_{ij} = \frac{d_i}{\alpha(T-t_{ij})}$ , a higher type  $\theta_{ij}$  indicates either a higher downlink demand  $d_i$ , or a longer travel time  $t_{ij}$ . In the first case, if the downlink demand  $d_i$  is higher, the employed UAV  $j$  must increase the transmit power to satisfy the larger communication needs. Therefore,  $p_j(\theta_{ij})$  will increase. On the other hand, if UAV  $j$  travel for a long time  $t_{ij}$  to arrive the service area of BS  $i$ , then more mobility energy is consumed during the movement.

In consequence, the unit payment  $u_i(\theta_{ij})$  should be increased accordingly, to compensate for the longer travel. Therefore, a UAV of a higher type is required to provide more available transmit power, and will be given a higher unit payment. The conclusion in Proposition 1 will lead to the necessary and sufficient conditions of a feasible contract, as shown next.

**Theorem 1.** *[Necessary and Sufficient Condition] For a contract set  $\Phi_i = \{(u_i(\theta_{ij}), p_j(\theta_{ij})) | \forall \theta_{ij}\}$ , it is feasible if and only if all the following three conditions hold: (a)  $\frac{dp_j(\theta_{ij})}{d\theta_{ij}} \geq 0$  and  $\frac{du_i(\theta_{ij})}{d\theta_{ij}} \geq 0$ , (b)  $\theta^{\min} u_i(\theta^{\min}) - p_j(\theta^{\min}) - M_{ij} \geq 0$ , (c)  $\frac{dp_j(\theta_{ij})}{d\theta_{ij}} = \theta_{ij} \cdot \frac{du_i(\theta_{ij})}{d\theta_{ij}}$ .*

*Proof.* See Appendix B. □

Theorem 1 gives the necessary and sufficient conditions for a contract set  $\Phi_i$  to be feasible. Therefore, each solution satisfying Theorem 1 guarantees that a UAV only accepts the contract designed for its own type, and provides the required transmit power to meet the downlink demand. Unfortunately, Theorem 1 results in a loose solution set, where an infinite number of feasible contracts exist. In order to find the most feasible solution, in this design, the simplest contract, where  $\frac{du_i(\theta_{ij})}{d\theta_{ij}} = \gamma_i > 0$ , is selected. This simple contract assignment leads to the least amount of data transmission and the shortest signal processing time, and thus, the requested UAV can be more rapidly deployed to serve the hotspot UEs. Therefore, in order to enable a short association stage, the simplest contract is the most adequate choice for practical uses. Consequently, the feasible contract that is proposed by BS  $i$  is given as follows.

**Lemma 1.** *Under the condition that  $\frac{du_i(\theta_{ij})}{d\theta_{ij}} = \gamma_i$ , the feasible contract between BS  $i$  and a UAV  $j$  of type  $\theta_{ij}$  is  $\phi_{ij} = (u_i, p_j) = (\gamma_i \theta_{ij}, \gamma_i \theta_{ij}^2 / 2)$ , where  $\gamma_i = \frac{2\alpha^2 T^2 p_h}{d_i^2}$ .*

*Proof.* Based on  $\frac{du_i(\theta_{ij})}{d\theta_{ij}} = \gamma_i$  and condition (c) of Theorem 1, we have  $u_i = \gamma_i \theta_{ij}$ ,  $p_j = \gamma_i \theta_{ij}^2 / 2$ , and condition (a) holds naturally. For BS  $i$ , the minimal UAV type is  $\theta^{\min} = \frac{d_i}{\alpha T}$ , when  $t_{ij} = 0$ . Therefore, condition (b) becomes  $\gamma_i \geq \frac{2M_{ij}}{\theta^{\min 2}} = \frac{2\alpha^2 T^2 p_h}{d_i^2}$ . Therefore, we set  $\gamma_i = \frac{2\alpha^2 T^2 p_h}{d_i^2}$ . □

Therefore, for each overloaded BS  $i$ , the designed contract is  $(u_i, p_j) = (\gamma_i \theta_{ij}, \gamma_i \theta_{ij}^2 / 2)$  with  $\gamma_i = \frac{2\alpha^2 T^2 p_h}{d_i^2}$  for each UAV in  $\mathcal{J}$  with any type  $\theta_{ij}$ .

### B. The optimal UAV association under the feasible contract

Given the feasible contract set  $\{(\gamma_i \theta_{ij}, \gamma_i \theta_{ij}^2 / 2) | \forall \theta_{ij}\}$ , the utility  $R_{ij}(\theta_{ij})$  of each candidate UAV  $j \in \mathcal{J}$  and the utility  $U_{ij}(\theta_{ij})$  of the requesting BS  $i$  can be jointly determined. Then, the

optimization problem in (12) becomes

$$\max_{j \in \mathcal{J}} U_{ij}(\theta_{ij}), \quad (21a)$$

$$\text{s. t. } p_{ij}(\mathbf{x}_{ij}^*, \rho_i^c) \leq p_j(\theta_{ij}) \leq \min\{p_{ij}^{\max}, p_{\max}\}, \quad (21b)$$

$$t_{ij} \leq \kappa_i T. \quad (21c)$$

Therefore, the last task is for BS  $i$  to find a UAV of the optimal type  $\theta_{ij}^*$  that maximizes its utility in (21a), while satisfying the constraints (21b) and (21c). However, since BS  $i$  does not know the type or the movement duration of each UAV  $j \in \mathcal{J}$ , problem (21) is not solvable, until more information is provided to BS  $i$ . Therefore, during the association stage, after BS  $i$  sends the request signal with  $\mathbf{x}_{ij}^*$ ,  $\kappa_i$ ,  $d_i$ , and  $\Phi_i$ , each UAV  $j$  will respond with its type  $\theta_{ij}$ . Ultimately, based on the responses, BS  $i$  can calculate the corresponding utility of each UAV, and employ the one that maximizes its own payoff. By substituting  $t_{ij}$ ,  $u_i$  and  $p_j$  with  $\theta_{ij}$ , we find that the derivation  $\frac{dU_{ij}(\theta_{ij})}{d\theta_{ij}} < 0$ . Therefore, the optimal UAV is  $j^* = \arg \max_{j \in \mathcal{J}_i} U(\theta_{ij}) = \arg \min_{j \in \mathcal{J}_i} \theta_{ij}$ , where  $\mathcal{J}_i = \{j | p_{ij}(\mathbf{x}_{ij}^*, \rho_i^c) \leq \frac{\gamma_i}{2} \theta_{ij}^2 \leq \min\{p_{ij}^{\max}, p_{\max}\}, t_{ij} \leq \kappa_i T\}$ . In other words, the qualified UAV with a smallest type will be the optimal solution. The complete process of the predictive UAV deployment process is summarized in Algorithm 1.

Compared with a conventional deployment approach in which a BS requests all necessary information from all UAVs, and then, solves the association problem via a centralized approach, the proposed algorithm is more efficient for practical implementation for three reasons. First, a centralized method requires all UAVs to send their locations and onboard energy to the BS, which is impractical. In contrast, our approach only requires the qualified UAVs to provide their types, thus yielding less information exchange in the communication phase. Second, given Lemma 1, the contract design costs no computation. As such, the optimal UAV is the UAV with the smallest type, which is easy to identify. Hence, the proposed approach is simpler for implementation, compared with a centralized method. Third, in the proposed algorithm, each UAV cannot benefit from misrepresenting on its location or onboard energy. This incentive mechanism guarantees a truthful information exchange between the BS and UAVs. Therefore, compared with a conventional centralized method, our proposed algorithm reduces the amount of data needed for the necessary communications during the association stage, exhibits a much lower complexity, and ensure a truthful information exchange between the BS and UAVs.

---

**Algorithm 1** Proposed process for the UAV predictive deployment
 

---

For each BS  $i \in \mathcal{I}$ , once downlink communication exceeds the network capacity, **do**:

**1. Learning stage:**

- (a) BS  $i$  collects  $\mathcal{S}_i$  to model the UE distribution  $f_i(\mathbf{y})$ , estimate the downlink traffic density  $S_i(\mathbf{y})$ , and detect the hotspot area  $\mathcal{A}_i^c$  based on the WEM approaches proposed in Section IV.
- (b) BS  $i$  calculates the downlink demand  $d_i$  of the offloaded UEs via (6), estimates the number  $N$  of required UAVs through (7), and computes the service point  $\mathbf{x}_{ij}^*$  for each target UAV  $j$ , based on the solution in [11].

**2. Association stage:** for  $n = 1, \dots, N$ :

- (a) BS  $i$  listens to the broadcast channel. If the channel is occupied, wait; otherwise, BS  $i$  broadcasts the request signal with  $d_i(n)$ ,  $\mathbf{x}_{ij}^*(n)$ ,  $\kappa_i$ , and  $\Phi_i(n) = \{\gamma_i \theta_{ij}, \frac{\gamma_i}{2} \theta_{ij}^2 | \forall \theta_{ij}\}$ , where  $\gamma_i = \frac{2\alpha^2 T^2 p_h}{d_i(n)^2}$ ;
- (b) Each UAV  $j \in \mathcal{J}$  listens the broadcast channel. After receiving the request from BS  $i$ , each UAV calculates the movement time  $t_{ij}$ , its UAV type  $\theta_{ij}$  with respect to BS  $i$ , and the available transmit power  $p_{ij}^{\max}$  after arriving at  $\mathbf{x}_{ij}^*$ . If  $p_{ij}^{\max} \geq \frac{\gamma_i}{2} \theta_{ij}^2$  and  $t_{ij} \leq \kappa_i T$ , UAV  $j$  replies  $\theta_{ij}$  to BS  $i$ ; otherwise, ignore.
- (c) BS  $i$  identifies the feasible UAV set  $\mathcal{J}_i$ , and employs the optimal UAV  $j^* = \arg \min_{j \in \mathcal{J}_i} \theta_{ij}$ .
- (d) If  $n = N$ , BS  $i$  releases the broadcast channel; otherwise, go back to 2(a).

**3. Movement stage:** The employed UAV  $j^*$  starts to move towards the service point of the requesting BS  $i$ .

**4. Service stage:**

- (a) BS  $i$  pays  $\gamma_i \theta_{ij^*} d_i$ , and offloads the UEs within  $\mathcal{A}_i^c$  to UAV  $j^*$ .
- (b) UAV  $j^*$  provides the downlink service with a transmit power  $p_{j^*} = \frac{\gamma_i}{2} \theta_{ij^*}^2$  for a service time  $T - t_{ij^*}$ .

**End**

When the service stage ends, the BS-UAV association terminates. Then, UAV  $j^*$  starts to listen to the broadcast channel, or moves to a recharging station if its on-board energy  $E_j$  is low.

---

## VI. SIMULATION RESULTS AND ANALYSIS

### A. Simulation parameters

For our simulations, we consider a UAV-assisted wireless network in a dense urban environment, operating at the 2 GHz frequency with a downlink bandwidth of 20 MHz. The parameters in the LOS probability model are  $a = 9.6$  and  $b = 0.28$  [28]. The Gaussian parameters of the additional air-to-ground path loss are  $\mu_{\text{LOS}} = 1.6$  and  $\sigma_{\text{LOS}} = 8.41$  for the LOS link while  $\mu_{\text{NLOS}} = 23$  and  $\sigma_{\text{NLOS}} = 33.78$  for the NLOS case [27]. For the UAV parameters [34], we set the mobility power  $m = 40$  W with an average moving speed of 5 m/s, and the hovering power is  $p_h = 10$  W. For each UAV, the maximal on-board energy is 40 Wh, the recharging time is 10

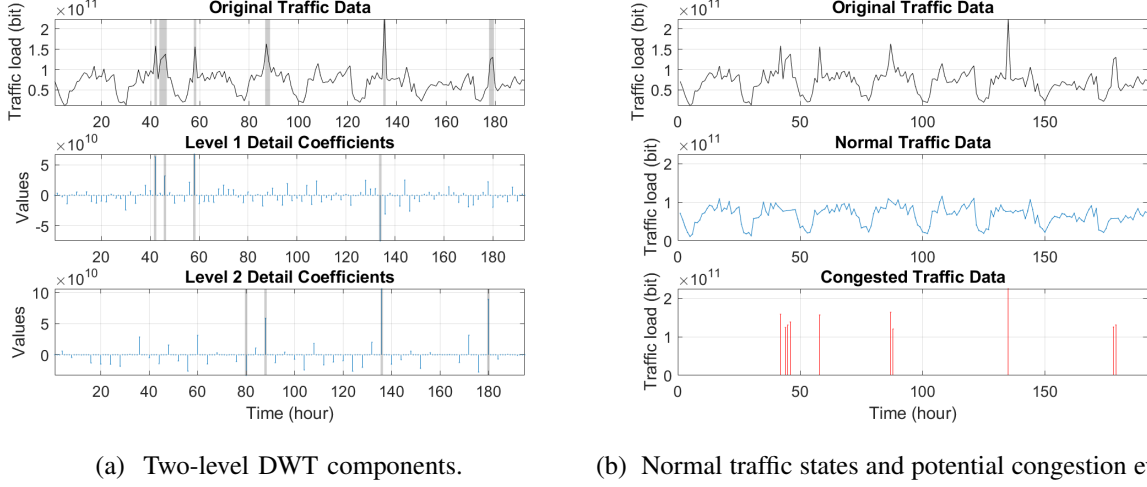


Fig. 3: Two-level DWT is applied to detect the cellular traffic congestion from a city level.

minutes, and battery recharge can be finished at a closest BS<sup>2</sup>. The maximum downlink transmit power of a UAV aerial BS is  $p_{\max} = 40$  W, and the unit cost of UAV's on-board energy is  $\alpha = 1$ . At each UE, the average noise power spectral density is  $-174$  dBm/Hz, and the price that UEs pays per bit of data is  $\beta = 10e - 7$ . For the UAV deployment process, we set  $\Delta T = 1$  second, and the learning duration  $\tau = 2$  minutes. The ratio of efficient transmission in each time slot is  $\eta = 90\%$ , and the maximum ratio of the UAV's movement duration over the time interval is  $\kappa_i = 0.5$ . Moreover, considering network congestion in a wireless cellular system lasts from a thousand seconds up to hours [35], we set  $T$  to be 18 minutes (1080 seconds), so that the offload service interval is shorter than the time period of common hotspot events.

### B. Dataset description and preprocessing

An open-source dataset “city-cellular-traffic-map” in [24] is used for the modeling, training, and testing of the proposed UAV deployment framework. The dataset collects HTTP traffic data through the cellular networks during each hour within a middle-sized city of China from August 19 to August 26, 2012. The dataset consist of two parts. One lists the identification number (ID) and the location in longitude and latitude of each BS, and the other collects the number of UEs, packets and traffic data (in bytes) that each BS transmits to downlink UEs during each hour of the aforementioned eight days. In order to identify hotspot events in the dataset, we apply the discrete wavelet transform (DWT) to the cellular traffic during each hour in the city level. As shown in the upper figure of Fig. 3, the cellular traffic within the city area presents a conspicuously periodic pattern, with several sudden and erratic surges. DWT processes the time-serial data by analyzing

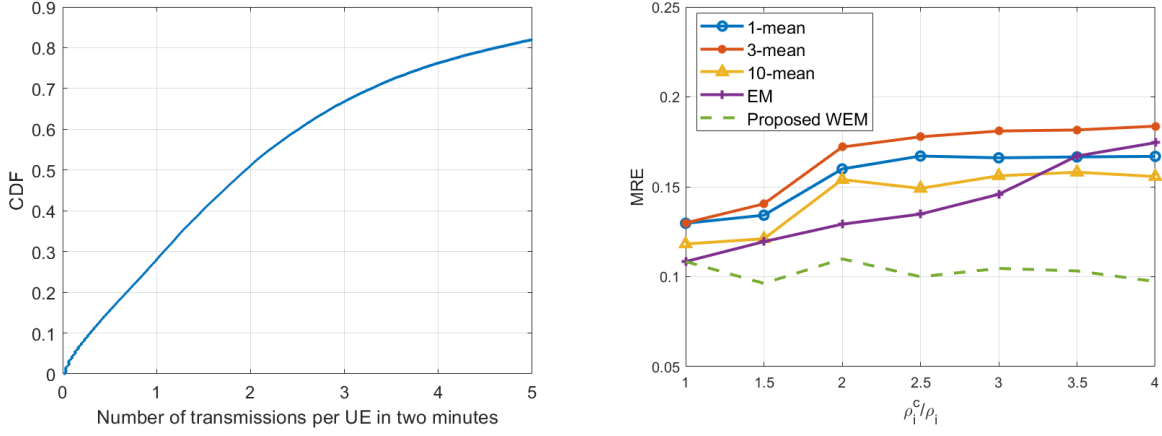
<sup>2</sup>The energy-efficient trajectory optimization for UAV power recharge will be subject to our future work.

both the value and frequency components, where the lower-frequency component defines the long term trend, and the higher-frequency component represents the small-scale rapid variation of the data. A hotspot event usually causes a steep surge in a cellular traffic amount. Therefore, such rapid change can be captured by DWT in the higher frequency domain. As shown in Fig. 3a, a two-level DWT is applied to detect the frequency change of the cellular traffic, and the gray bars mark the time points when the traffic amount has a sudden increase. Based on the result, the dataset is separated into the normal traffic data and the potential congested traffic, as given in Fig. 3b. Here, we find a time window from 42 to 47, which is 18 to 23 p.m. on August 20, that shows a continuously high cellular traffic amount, and the hotspot event is highly likely to happen in the city during this period. Therefore, the traffic data from 42 to 47 are selected to study the predictive UAV deployment in the following analysis.

However, the data in [24] does not include the location information of each connected UE, or the service area of each BS. In order to identify the UE distribution and the downlink traffic density, the location and time labels are generated and attached to each downlink transmission record via the following approach. First, the service area  $\mathcal{A}_i$  of each BS  $i$  is partitioned, based on the closest-distance principle. Next, we use the total packet number to denote the number of downlink transmissions. Furthermore, we note that the original time label  $t$  in [24] is based on one hour, which is too coarse to enable our analysis. Therefore, in order to extract the estimated data with a desired duration, a new label with a finer time grain of one second is randomly generated and attached to each traffic record. Then, given  $\tau = 2$  and  $T = 18$ , we divide each hour evenly into three intervals, such that the cellular data during first two minutes of each interval is used to model the spatial distribution of UEs and downlink traffic, and data from the following 18 minutes is used to estimate the transmission performance of the UAV BS, as well to validate the accuracy of the proposed learning algorithm. Eventually, the location label  $\mathbf{y}_n$  of each traffic record is generated by a GMM with random parameters to which we add a zero-mean Gaussian noise. The variance of the Gaussian noise is set as three meters, which is the average error of the GPS location for common mobile equipments. With the additional location and time information, the dataset is suitable for the studied problem.

### C. Performance of the cellular traffic prediction

Given that each overloaded BS  $i$  takes  $\tau = 2$  minutes to collect the transmission records  $\mathcal{S}_i$ , in order to guarantee that the training dataset  $\mathcal{S}_i$  is representative, we assume that each



(a) CDF of the number of transmissions per UE per two minutes. (b) MRE of the proposed WEM approach and baselines of the EM and  $k$ -mean methods.

Fig. 4: Statistical results and prediction errors in the learning stage.

UE will have at least one downlink transmission during the learning stage. This assumption is supported by the analysis result in Fig. 4a, which shows that over 70% UEs receive, on average, one packet within every two minutes. Based on the collected dataset  $\mathcal{S}_i$ , the proposed WEM approach is applied to predict the data demand  $d_i$  within the hotspot area  $\mathcal{A}_i^c$ , while the actual traffic demand  $d_i^{\text{actual}}$  is calculated by summing up the real transmission amount within  $\mathcal{A}_i^c$  during the following service time  $T$ . In order to evaluate the performance of the traffic prediction, the mean relative error (MRE) is applied as a metric where  $\delta_{\text{MRE}} = \mathbb{E}_{i,t}[\frac{|d_i - d_i^{\text{actual}}|}{d_i^{\text{actual}}}]$ . For comparison purposes, we introduce the conventional EM and  $k$ -mean methods as baselines. Note that, the EM method has been used in Section IV-A for modeling the UE distribution  $f_i(\mathbf{y})$ . Then, the predicted traffic demand resulting from the EM method will be  $d_i^{\text{EM}} = T \cdot \mathbb{E}_n(s_n) \cdot \int_{\mathbf{y} \in \mathcal{A}_i^c} f_i(\mathbf{y}) d\mathbf{y}$ , where  $\mathbb{E}_n(s_n) = \frac{\sum_n s_n \Delta t}{\tau}$  is the time average of the summed data rate towards all UEs, and  $\int_{\mathbf{y} \in \mathcal{A}_i^c} f_i(\mathbf{y}) d\mathbf{y}$  is the percentage of UEs within the hotspot area. On the other hand, the  $k$ -mean method predicts the traffic density by averaging the local information from  $k$  closest neighbors. We repeat the simulation for 1000 times. In each run, the location and time labels of each transmission record are generated randomly.

Fig. 4b shows the prediction MRE of the WEM, EM and  $k$ -mean methods, where  $k = 1, 3$  and 10, as the average data demand  $\rho_i^c$  of the hotspot UEs increases. When  $\frac{\rho_i^c}{\rho_i} = 1$ , each hotspot UE will have the same data demand as the other UEs in the network. In this case, the WEM and EM approaches yield a similar prediction accuracy with an MRE of 11%, and the prediction errors of  $k$ -mean methods are between 12% and 12.5%. Note that, a prediction error of 11% yields lower than 0.1 W of deviation on the value of  $p_{ij}(\mathbf{x}_{ij}^*, \rho_i)$ . Clearly, this is a very small

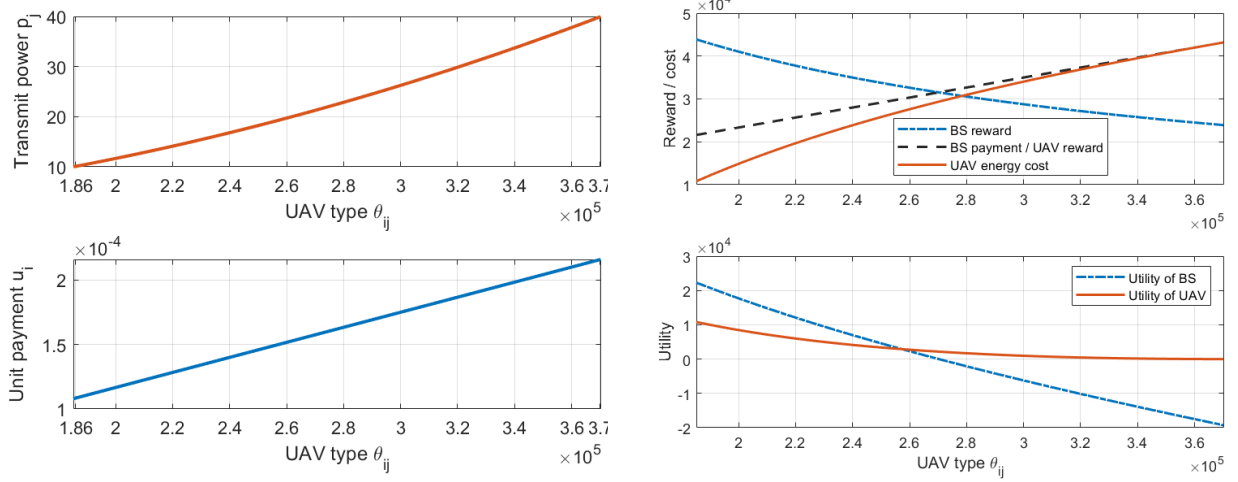
value compared to the hovering and transmit powers of a typical UAV. When the traffic load within different regions of the cellular network becomes more uneven, the prediction error of WEM remains the same, while the errors of the EM and  $k$ -mean methods gradually increase above 15.5%. Clearly, for  $\frac{\rho_i^c}{\rho_i} > 1$ , the proposed WEM approach outperforms all other baselines.

In the WEM approach, the traffic density  $\bar{S}_i(\mathbf{y})$  of each location  $\mathbf{y}$  is considered when optimizing the prediction parameters. Therefore, the spatial feature of downlink transmissions can be accurately captured, and the performance of WEM does not decrease when the traffic load in the cellular system becomes uneven. However, the EM model only considers the location information, but ignores the downlink rate of each transmission. Therefore, when the traffic demand shows distinct patterns in different regions, the EM method fails to capture the spatial diversity, and its prediction error increases significantly. Given that the  $k$ -mean method predicts the cellular traffic by averaging data from  $k$  closest neighbors, it captures the traffic spatial difference from local information. However, as the cellular traffic becomes more uneven, the local information is more sensitive to the noise, and thus, the prediction errors of  $k$ -mean methods increase, as  $\rho_i^c$  increases. By comparing different  $k$ -mean algorithms, we find that 3-mean achieves the worst performance, because information from three neighbors is not sufficient to cancel out the noise. The simulation results also show that the average information from 10 neighbors is sufficient to provide a robust traffic prediction, and thus, 10-mean yields the best performance among all  $k$ -mean methods. Meanwhile, when the ratio  $\frac{\rho_i^c}{\rho_i}$  is small, EM yields a lower error rate compared to  $k$ -mean; however, as  $\frac{\rho_i^c}{\rho_i} \geq 3.5$ , EM will result in a higher prediction error compared with 1-mean and 10-mean. Since the  $k$ -mean method can capture the traffic diversity, its prediction error no longer increases after the ratio exceeds 2.5. Due to the lack of traffic information, EM eventually results in a larger error than  $k$ -mean when  $\frac{\rho_i^c}{\rho_i} > 3.5$ .

#### D. Performance of the designed contracts

In this section, we study the performance of the designed contract by evaluating the individual utilities of a BS and its associated UAV. The contract is designed based on Lemma 1 by a BS with ID 7939, using the data from time 42 in [24]. Fig. 5a shows the relationship between the type of the associated UAV with the transmit power and the unit payment in the contract. As the UAV type  $\theta_{ij}$  increases, both the transmit power  $p_j$  and the unit payment  $u_i$  in the contract will increase. This result supports the conclusion of Proposition 1, where a UAV of a higher type is required to provide more transmit power and will be given a higher unit payment. Fig. 5b



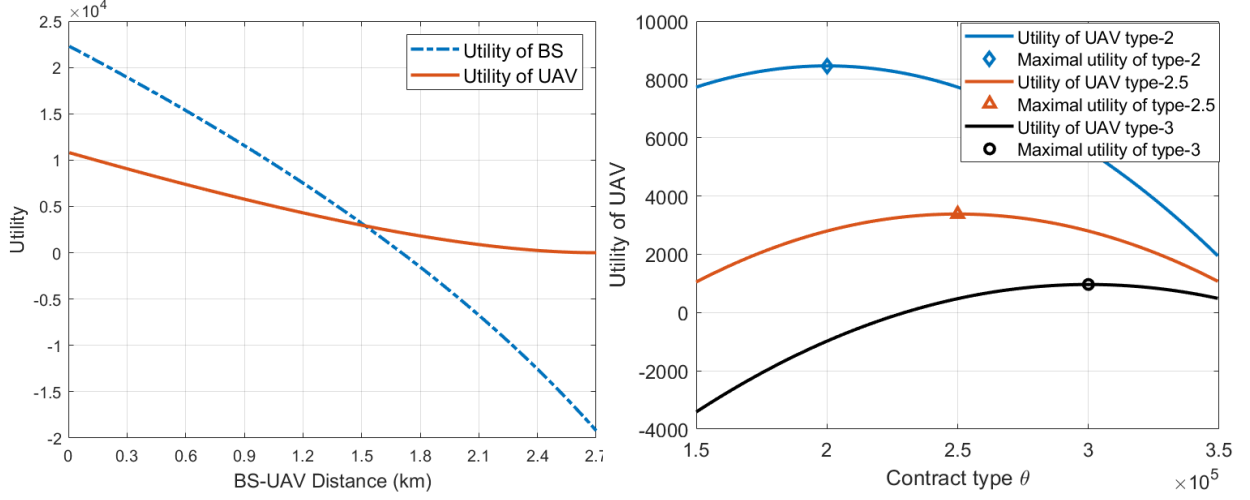


(a) Transmit power and unit payment, given different (b) Costs, rewards and overall utilities of the associated UAV types. BS and UAV, given different UAV types.

Fig. 5: As the UAV type increases, the transmit power and the unit payment both increase. However, the overall utilities of the associated BS and UAV will decrease.

investigates the relationship between the UAV type and the reward, cost, as well as the overall utilities of the requesting BS and the deployed UAV, respectively. First, as the UAV type  $\theta_{ij}$  becomes larger, although the transmit power  $p_j(\theta_{ij})$  increases, the BS's reward  $\beta B_{ij}(p_j)$  from the downlink UEs will decrease. Note that, given the downlink demand  $d_i$  fixed, a higher UAV type  $\theta_{ij}$  results in a longer travel time  $t_{ij}$ . By substituting  $t_{ij}$  with  $\theta_{ij}$  in (8), we find that the derivation  $\frac{dB_{ij}(\theta_{ij})}{d\theta_{ij}} < 0$ . Therefore, the BS's reward  $\beta B_{ij}(\theta_{ij})$  will decrease as the UAV type  $\theta_{ij}$  increases. Moreover, as shown in Fig. 5b, a higher UAV type results in a higher payment  $u_i(\theta_{ij})d_i$  from BS  $i$  to UAV  $j$ . Therefore, the utility of BS  $i$  will be lower for a larger  $\theta_{ij}$ . For the deployed UAV  $j$ , a larger type  $\theta_{ij}$  leads to a higher reward  $u_i(\theta_{ij})d_i$  from BS  $i$ , but meanwhile, the energy cost will increase, due to a longer movement time  $t_{ij}$  and a higher transmit power  $p_i$ . Furthermore, as shown in Fig. 5b, the energy cost increases faster than the economic benefit. Thus, the utility of the deployed UAV will also decrease, as  $\theta_{ij}$  becomes larger.

Next, we study the relationship between the BS-UAV distance and the individual utilities of the BS and its associated UAV. As shown in Fig. 6a, if the distance between a BS and its employed UAV becomes larger, the utilities of the UAV and the BS will both decrease, because a longer BS-UAV distance results in a larger movement time  $t_{ij}$  and a higher UAV type  $\theta_{ij}$ . Since the unit payment  $u_i(\theta_{ij})$  of the BS will increase to compensate for the UAV's mobility power over the longer distance, the utility of BS  $i$  becomes negative, when the distance is larger than 1.7 km. On the other hand, for the employed UAV, as the movement distance becomes larger,



(a) Utilities of BS and UAV, given different distances. (b) Utilities of UAVs, given different contract types.

Fig. 6: The designed contract ensures the employed UAV to receive a non-negative payoff, and the highest utility is achieved by accepting the contract of its own type.

more power will be consumed during the movement stage and more transmit power is required during the service stage. Therefore, the utility of UAV decreases with the increase of the moving distance. However, due to the IR condition, the payment from the BS will increase accordingly. Fig. 6a shows that the UAV's utility is always non-negative. Therefore, we can conclude that the IR condition holds in the designed contract in Lemma 1. Fig. 6b investigates how the IC condition holds in the designed contract. The utilities of three UAVs, where their actual types are  $2 \times 10^5$  (type-2),  $2.5 \times 10^5$  (type-2.5), and  $3 \times 10^5$  (type-3), is shown in Fig. 6b, when they accept different kinds of contracts from BS 7939. As shown in Fig. 6b, the maximum utility of each UAV is achieved when the accepted contract is of its own type. Therefore, the IC condition holds, and the designed contract set of Lemma 1 is feasible.

An interesting observation on the utility function is that the prediction error of  $d_i$  does not cause small fluctuations on the utility value of the BS or the employed UAV. Although  $d_i$  determines the type  $\theta_{ij}$  of each UAV and the value of  $\gamma_i$ , after expanding the expressions of utility functions, we find that the transmit power is  $p_j = \gamma_i \theta_{ij}^2 / 2 = \frac{mT^2}{4\alpha(T-t_{ij})^2}$  and the total payment from BS  $i$  to the employed UAV  $j$  is  $u_i d_i = \gamma_i \theta_{ij} d_i = \frac{mT^2}{2(T-t_{ij})}$ . Therefore,  $d_i$  no longer appears in the formulas, and an inaccuracy in  $d_i$  will not impact the utility functions in (9) and (10). The main effect of  $d_i$  in the predictive UAV deployment is to determine the minimum required transmit power  $p_{ij}(\mathbf{x}_{ij}^*, \rho_i^c)$ . If the predicted demand  $d_i$  is much lower than the real data demand, then  $p_{ij}(\mathbf{x}_{ij}^*, \rho_i^c)$  will be smaller. In consequence, some UAVs without enough energy may be inappropriately considered to be a qualified choice, and might be employed. On the other

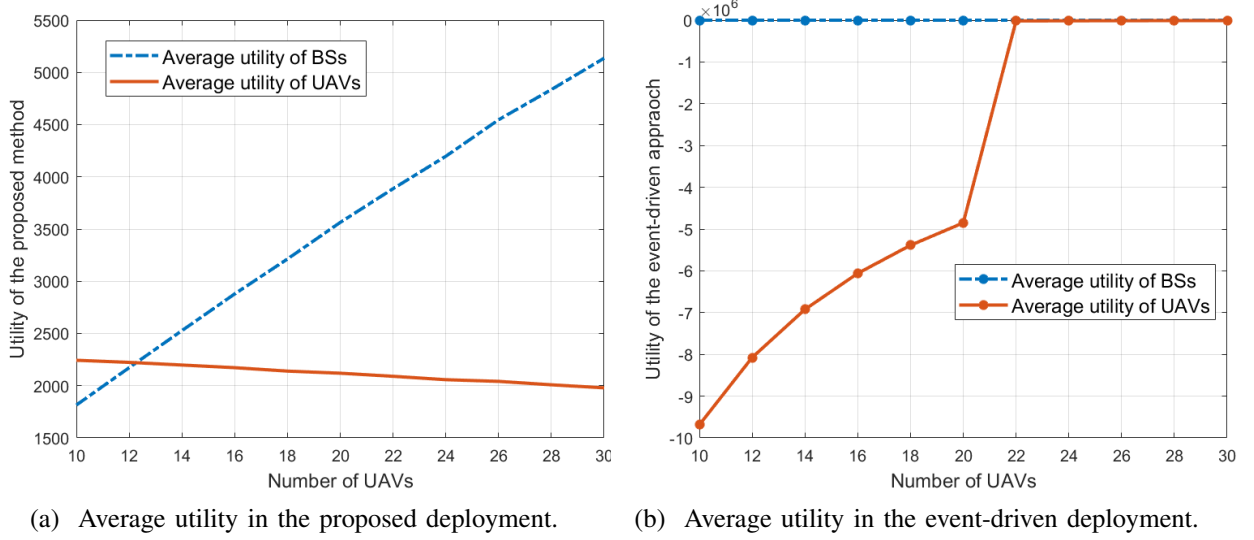


Fig. 7: Average utilities of BSs and UAVs, given different numbers of available UAVs in the network.

hand, if  $d_i$  is much higher than the actual demand, some qualified UAVs with enough power may be excluded from the candidate set  $\mathcal{J}_i$ . Both cases can lead to a suboptimal solution to (12). However, as long as the error on  $d_i$  causes no change to the association result, the utilities of BS  $i$  and the employed UAV will always be accurate. Based on this observation, the proposed approach is highly robust to prediction errors.

#### E. Evaluation of the predictive UAV deployment

In Fig. 7, we evaluate the performance of the proposed UAV deployment method, by comparing it with an event-driven allocation approach, which requests the closest UAV every time the downlink congestion occurs, without the prediction on traffic demand or the feasible contract design. In the event-driven approach, the unit payment  $u_i$  from BS  $i$  to the employed UAV equals to the unit price  $\beta$  from downlink UEs. In return, the employed UAV  $j$  provides the downlink service to the best of its power ability, where  $p_j = \min\{p_{ij}(\mathbf{x}_{ij}^*, \rho_i), p_{ij}^{\max}, p_{\max}\}$ . The traffic data from time 42 to 43 in [24] is used to evaluate the performance of two approaches. We repeat the simulation for 1000 times. In each run, the initial location and on-board energy of each UAV, as well as the location and time label of each transmission record, are generated randomly.

First, Fig. 7a shows that the average utilities of both the overloaded BSs and the employed UAVs, resulting from the proposed approach, will be positive. As the number of available UAVs increases, each overloaded BS have more options to offload its excess downlink traffic and maximize its utility. Thus, the average utility of each BS will increase, given more available UAVs. On the other hand, since the number of overloaded BSs is around 21, the number of

employed UAVs will be fixed near 21. In consequence, as more UAVs is available, the average utility of each UAV naturally decreases. However, the total utility of all UAVs becomes larger. Given more UAVs distributed in the network, the average distance between each overloaded BS and its employed UAV will decrease. Therefore, less energy is consumed during the movement stage, and the aerial cellular service can be provided to the UEs with a shorter delay. In consequence, the total utility of the BS and UAV groups both increase in the proposed deployment method, as the number of available UAVs increases. However, in the event-driven method, as shown in Fig. 7b, the average utility of each overloaded BS is always zero, and the utility of each UAV is negative. Since each BS gives all its income from downlink UEs to the employed UAV, the utility of each BS is always zero. On the other hand, without a proper prediction on the UE distribution and traffic demand, the employed UAV in the event-driven approach must change its location constantly to meet the on-demand transmission need. Therefore, a lot of energy will be consumed by mobility, and the overall utility for each UAV is always negative. Furthermore, given the number of overloaded BSs is around 21, the average utility of each UAV increases dramatically, when the number of UAVs changes from 20 to 22. When the number of UAVs is smaller than BSs, the travel distance of each UAV to the associated BS is usually large, and a lot of energy is consumed during the mobility stage. Although each BS gives all the payment from UEs to the employed UAV, in the most cases, the payment cannot offset the energy cost of each UAV. As the number of UAVs is greater than BSs, such problem becomes less serious. However, the average utility of each UAV is still negative.

From Fig. 7, we can conclude that, the event-driven approach fails to be a practical solution to the considered UAV deployment problem, because the negative revenue will discourage UAV operators from providing aerial cellular service. However, in the proposed UAV deployment approach, due to the designed contract, a sufficient payment is provided to the employed UAV to reward its aerial cellular service, and the downlink data demand within the hotspot area can be satisfied. Therefore, both the BS and UAV operators can receive positive revenues. Furthermore, simulation results show that the UAV's recharging frequency in the proposed approach is around 50% higher than the event-driven method. Therefore, the proposed approach enables each UAV to use its on-board energy more efficiently to serve the hotspot UEs with downlink communications, and shows a significant advantage on the economical revenues of both the BS and UAV networks, compared with the baseline, event-driven approach.

## VII. CONCLUSION

In this paper, we have proposed a novel approach for predictive deployment of UAV base stations to complement the ground cellular system in face of the hotspot events. In particular, four inter-related and sequential stages have been proposed to enable the ground BS to optimally employ a UAV to offload the excess downlink traffic. First, a novel framework, based on the EM and WEM methods, has been proposed to estimate the UE distribution and the downlink traffic demand. Next, to guarantee a truthful information exchange between the BS and UAV operators, a traffic offload contract have been developed, and the sufficient and necessary conditions for having a feasible contract have been analytically derived. Then, an optimization problem have been formulated to deploy the optimal UAV onto the hotspot area in a way that the utility of each overloaded ground BS is maximized. Simulation and analytical results show that the proposed WEM approach yields a prediction error around 10%, and compared with the EM and  $k$ -mean schemes, the proposed WEM algorithm yields a higher prediction accuracy, particularly when the traffic load in the cellular system becomes spatially uneven. Furthermore, compared with a baseline, event-driven allocation method, the proposed predictive deployment approach enables UAV operators to provide efficient downlink service for hotspot users, and significantly improves the revenues of both the BS and UAV networks.

## APPENDIX A

### PROOF OF PROPOSITION 1

We first use contradiction to prove the proposition that if  $\theta_{ij} > \theta'_{ij}$ , then  $u_i(\theta_{ij}) \geq u_i(\theta'_{ij})$ . Then, we prove that if  $u_i(\theta_{ij}) \geq u_i(\theta'_{ij})$ , then  $p_j(\theta_{ij}) \geq p_j(\theta'_{ij})$ . Suppose that there exists  $u_i(\theta_{ij}) < u_i(\theta'_{ij})$ , but  $\theta_{ij} > \theta'_{ij}$ . Then, we have

$$\theta_{ij}u_i(\theta'_{ij}) + \theta'_{ij}u_i(\theta_{ij}) > \theta_{ij}u_i(\theta_{ij}) + \theta'_{ij}u_i(\theta'_{ij}). \quad (22)$$

On the other hand, from IC condition, we have

$$\theta_{ij}u_i(\theta_{ij}) - p_j(\theta_{ij}) \geq \theta_{ij}u_i(\theta'_{ij}) - p_j(\theta'_{ij}), \quad \theta'_{ij}u_i(\theta'_{ij}) - p_j(\theta'_{ij}) \geq \theta'_{ij}u_i(\theta_{ij}) - p_j(\theta_{ij}). \quad (23)$$

By adding the inequations in (23), we have  $\theta_{ij}u_i(\theta_{ij}) + \theta'_{ij}u_i(\theta'_{ij}) \geq \theta_{ij}u_i(\theta'_{ij}) + \theta'_{ij}u_i(\theta_{ij})$ , which contradicts to (22). This completes the first part of the proof.

Next, we prove that if  $u_i(\theta_{ij}) \geq u_i(\theta'_{ij})$ ,  $p_j(\theta_{ij}) \geq p_j(\theta'_{ij})$ . From the IC condition, we have  $\theta'_{ij}u_i(\theta'_{ij}) - p_j(\theta'_{ij}) \geq \theta'_{ij}u_i(\theta_{ij}) - p_j(\theta_{ij})$ , i.e.  $p_j(\theta_{ij}) - p_j(\theta'_{ij}) \geq \theta'_{ij}(u_i(\theta_{ij}) - u_i(\theta'_{ij}))$ . Since

$u_i(\theta_{ij}) > u_i(\theta'_{ij})$ , we conclude  $p_j(\theta_{ij}) - p_j(\theta'_{ij}) \geq \theta'_{ij} (u_i(\theta_{ij}) - u_i(\theta'_{ij})) \geq 0$ , and thus  $p_j(\theta_{ij}) \geq p_j(\theta'_{ij})$ . This completes the proof.

## APPENDIX B

### PROOF OF THEOREM 1

For notation simplicity, in this section, we denote  $u_i, p_j, \theta_{ij}, M_{ij}$  as  $u, P, \theta, M$  respectively.

#### A. Proof for necessary conditions

Given the IR and IC conditions, we prove Theorem 1 in this section. First, as shown in Proposition 1, for any  $\theta, \theta' \in \Theta$ , once  $\theta > \theta'$ , then  $u(\theta) \geq u(\theta')$  and  $P(\theta) \geq P(\theta')$ . Therefore, condition (a) of Theorem 1 is proved by Proposition 1. Second, condition (b) of Theorem 1 is supported by the IR condition, where  $R_{ij}(\theta) \geq 0$  for all  $\theta$  in  $\Theta$ , which naturally includes  $\theta^{\min}$ . Next, we prove condition (c). Let  $\Delta\theta = \theta' - \theta$ . According to the IC condition, for any  $\Delta\theta \in [\theta^{\min} - \theta^{\max}, 0) \cup (0, \theta^{\max} - \theta^{\min}]$ , we have:  $\theta \cdot u(\theta) - P(\theta) \geq \theta \cdot u(\theta + \Delta\theta) - P(\theta + \Delta\theta)$ , i.e.,  $\theta \cdot [u(\theta) - u(\theta + \Delta\theta)] \geq P(\theta) - P(\theta + \Delta\theta)$ . If  $\Delta\theta > 0$ , then according to Proposition 1,  $u(\theta + \Delta\theta) \geq u(\theta)$  and  $P(\theta + \Delta\theta) \geq P(\theta)$ . Here, we exclude the situation where  $u(\theta + \Delta\theta) = u(\theta)$  and  $P(\theta + \Delta\theta) = P(\theta)$  in the following discussion of this proof, because condition (c) naturally holds in this case. Therefore, for any  $\Delta\theta \in (0, \theta^{\max} - \theta^{\min}]$ , we have

$$\theta \leq \frac{P(\theta + \Delta\theta) - P(\theta)}{u(\theta + \Delta\theta) - u(\theta)}. \quad (24)$$

If  $\Delta\theta < 0$ , then  $u(\theta + \Delta\theta) < u(\theta)$  and  $P(\theta + \Delta\theta) < P(\theta)$ . Thus, for any  $\Delta\theta \in [\theta^{\min} - \theta^{\max}, 0)$ ,

$$\theta \geq \frac{P(\theta + \Delta\theta) - P(\theta)}{u(\theta + \Delta\theta) - u(\theta)}. \quad (25)$$

Combing (24) and (25), we have  $\frac{dP}{d\theta} / \frac{du}{d\theta} = \lim_{\Delta\theta \rightarrow 0} \frac{P(\theta + \Delta\theta) - P(\theta)}{u(\theta + \Delta\theta) - u(\theta)} = \theta$ , which proves condition (c) of Theorem 1.

#### B. Proof for sufficient conditions

From Theorem 1, we will prove the IR and IC conditions in this section. First, we prove the IR condition. According to condition (b) of Theorem 1,  $\theta^{\min}$  satisfies the IR condition. Then, we prove that for any  $\theta \in (\theta^{\min}, \theta^{\max}]$ , the IR condition holds. From condition (c) of Theorem 1, we have the following inequalities,  $\frac{P(\theta) - P(\theta^{\min})}{u(\theta) - u(\theta^{\min})} \leq \theta$ , i.e.,

$$P(\theta^{\min}) \geq P(\theta) - \theta \cdot [u(\theta) - u(\theta^{\min})]. \quad (26)$$

From condition (b), we have

$$\theta^{\min} \cdot u(\theta^{\min}) - P(\theta^{\min}) - M \geq 0. \quad (27)$$

By combining (26) and (27), we have  $\theta \cdot u(\theta) - P(\theta) - M \geq (\theta - \theta^{\min}) \cdot u(\theta^{\min}) \geq 0$ . Thus, for any  $\theta \in \Theta$ , the IR condition holds.

In the end, we prove the IC condition. Let  $h = \theta \cdot u(\theta) - P(\theta) - M - [\theta \cdot u(\theta') - P(\theta') - M]$ . And we prove that  $h \geq 0$ . From condition (c), we have, if  $\theta' > \theta$ , then  $\frac{P(\theta') - P(\theta)}{u(\theta') - u(\theta)} \geq \min\{\theta, \theta'\} = \theta$ . i.e.,  $P(\theta') - P(\theta) \geq \theta \cdot [u(\theta') - u(\theta)]$ . Therefore,  $h = \theta \cdot [u(\theta) - u(\theta')] + P(\theta') - P(\theta) \geq 0$ . On the other hand, if  $\theta' < \theta$ , then  $\frac{P(\theta) - P(\theta')}{u(\theta) - u(\theta')} \leq \max\{\theta, \theta'\} = \theta$ . i.e.,  $P(\theta) - P(\theta') \leq \theta \cdot [u(\theta) - u(\theta')]$ . Therefore,  $h \geq 0$ . Consequently, the IC condition holds.

## REFERENCES

- [1] Q. Zhang, M. Mozaffari, W. Saad, M. Bennis, and M. Debbah, "Machine learning for predictive on-demand deployment of UAVs for wireless communications," in *Proc. of IEEE Global Communications Conference*, Abu Dhabi, UAE, Dec 2018.
- [2] M. Mozaffari, W. Saad, M. Bennis, and M. Debbah, "Mobile unmanned aerial vehicles (UAVs) for energy-efficient Internet of Things communications," *IEEE Transactions on Wireless Communications*, vol. 16, no. 11, pp. 7574–7589, Sep 2017.
- [3] R. I. Bor-Yaliniz, A. El-Keyi, and H. Yanikomeroglu, "Efficient 3-D placement of an aerial base station in next generation cellular networks," in *Proc. of IEEE International Conference on Communications*, Kuala Lumpur, Malaysia, May 2016.
- [4] X. Zhang and L. Duan, "Fast deployment of UAV networks for optimal wireless coverage," *IEEE Transactions on Mobile Computing*, vol. 18, no. 3, pp. 588–601, May 2018.
- [5] W. Khawaja, I. Guvenc, D. Matolak, U.-C. Fiebig, and N. Schneckenberger, "A survey of air-to-ground propagation channel modeling for unmanned aerial vehicles," *IEEE Communications Surveys and Tutorials (Early Access)*, May 2019.
- [6] M. Mozaffari, W. Saad, M. Bennis, Y.-H. Nam, and M. Debbah, "A tutorial on UAVs for wireless networks: Applications, challenges, and open problems," *IEEE Communications Surveys and Tutorials*, to appear, 2019.
- [7] M. Mozaffari, A. T. Z. Kasgari, W. Saad, M. Bennis, and M. Debbah, "Beyond 5G with UAVs: Foundations of a 3D wireless cellular network," *IEEE Transactions on Wireless Communications*, vol. 18, no. 1, pp. 357–372, Jan 2018.
- [8] W. Saad, M. Bennis, and M. Chen, "A vision of 6G wireless systems: Applications, trends, technologies, and open research problems," *IEEE Network*, to appear, 2019.
- [9] M. Chen, U. Challita, W. Saad, C. Yin, and M. Debbah, "Artificial neural networks-based machine learning for wireless networks: A tutorial," *IEEE Communications Surveys and Tutorials*, to appear, 2019.
- [10] Z. Hu, Z. Zheng, L. Song, T. Wang, and X. Li, "UAV offloading: Spectrum trading contract design for UAV assisted cellular networks," *IEEE Transactions on Wireless Communications*, vol. 17, no. 9, pp. 6093–6107, July 2018.
- [11] M. Mozaffari, W. Saad, M. Bennis, and M. Debbah, "Optimal transport theory for power-efficient deployment of unmanned aerial vehicles," in *Proc. of IEEE International Conference on Communications*, Kuala Lumpur, Malaysia, May 2016.
- [12] E. Kalantari, H. Yanikomeroglu, and A. Yongacoglu, "On the number and 3D placement of drone base stations in wireless cellular networks," in *Proc. of IEEE 84th Vehicular Technology Conference*, Montreal, QC, Canada, Sep 2016.
- [13] J. Lyu, Y. Zeng, and R. Zhang, "UAV-aided offloading for cellular hotspot," *IEEE Transactions on Wireless Communications*, vol. 17, no. 6, pp. 3988–4001, Mar 2018.

- [14] V. Sharma, M. Bennis, and R. Kumar, "UAV-assisted heterogeneous networks for capacity enhancement," *IEEE Communications Letters*, vol. 20, no. 6, pp. 1207–1210, Apr 2016.
- [15] J. Lyu, Y. Zeng, and R. Zhang, "Spectrum sharing and cyclical multiple access in UAV-aided cellular offloading," in *Proc. of IEEE Global Communications Conference*, Singapore, Dec 2017.
- [16] F. Cheng, S. Zhang, Z. Li, Y. Chen, N. Zhao, R. Yu, and V. C. Leung, "UAV trajectory optimization for data offloading at the edge of multiple cells," *IEEE Transactions on Vehicular Technology*, vol. 67, no. 7, pp. 6732 – 6736, Mar 2018.
- [17] S. Sharafeddine and R. Islambouli, "On-demand deployment of multiple aerial base stations for traffic offloading and network recovery," *arXiv preprint arXiv:1807.02009*, 2018.
- [18] R. Li, Z. Zhao, J. Zheng, C. Mei, Y. Cai, and H. Zhang, "The learning and prediction of application-level traffic data in cellular networks," *IEEE Transactions on Wireless Communications*, vol. 16, no. 6, pp. 3899–3912, Mar 2017.
- [19] C. Yu, Y. Liu, D. Yao, L. T. Yang, H. Jin, H. Chen, and Q. Ding, "Modeling user activity patterns for next-place prediction," *IEEE Systems Journal*, vol. 11, no. 2, pp. 1060–1071, July 2017.
- [20] P. Valente Klaine, M. A. Imran, O. Onireti, and R. D. Souza, "A survey of machine learning techniques applied to self organizing cellular networks," *IEEE Communications Surveys and Tutorials*, vol. 19, no. 4, pp. 2392–2431, July 2017.
- [21] M. Chen, W. Saad, and C. Yin, "Liquid state machine learning for resource and cache management in LTE-U unmanned aerial vehicle (UAV) networks," *IEEE Transactions on Wireless Communications*, vol. 18, no. 3, pp. 1504 –1517, Jan 2019.
- [22] J. Chen, U. Yatnalli, and D. Gesbert, "Learning radio maps for UAV-aided wireless networks: A segmented regression approach," in *Proc. of IEEE International Conference on Communications*, Paris, France, May 2017.
- [23] R. Amorim, J. Wigard, H. Nguyen, I. Z. Kovacs, and P. Mogensen, "Machine-learning identification of airborne UAV-UEs based on LTE radio measurements," in *Proc. of IEEE Globecom Workshops*, Singapore, Jan 2017.
- [24] "City cellular traffic map," <https://github.com/caesar0301/city-cellular-traffic-map>, accessed: 2016-10-05.
- [25] P. Bolton and M. Dewatripont, *Contract theory*. MIT press, 2005.
- [26] L. Zhu, J. Zhang, Z. Xiao, X. Cao, D. O. Wu, and X.-G. Xia, "3D beamforming for flexible coverage in millimeter-wave uav communications," *IEEE Wireless Communications Letters*, 2019.
- [27] A. Al-Hourani, S. Kandeepan, and A. Jamalipour, "Modeling air-to-ground path loss for low altitude platforms in urban environments," in *Proc. of IEEE Global Communications Conference*, Austin, TX, USA, Dec 2014.
- [28] A. Al-Hourani, S. Kandeepan, and S. Lardner, "Optimal LAP altitude for maximum coverage," *IEEE Wireless Communications Letters*, vol. 3, no. 6, pp. 569–572, July 2014.
- [29] J. Lyu, Y. Zeng, and R. Zhang, "Cyclical multiple access in UAV-aided communications: A throughput-delay tradeoff," *IEEE Wireless Communications Letters*, vol. 5, no. 6, pp. 600–603, Aug 2016.
- [30] Y. Zeng, J. Xu, and R. Zhang, "Energy minimization for wireless communication with rotary-wing UAV," *IEEE Transactions on Wireless Communications*, vol. 18, no. 4, pp. 2329 – 2345, 2019.
- [31] A. T. Z. Kasgari, W. Saad, and M. Debbah, "Human-in-the-loop wireless communications: Machine learning and brain-aware resource management," *IEEE Transactions on Communications*, to appear, 2019.
- [32] B. Selim, O. Alhussein, S. Muhaidat, G. K. Karagiannidis, and J. Liang, "Modeling and analysis of wireless channels via the mixture of Gaussian distribution," *IEEE Transactions on Vehicular Technology*, vol. 65, no. 10, pp. 8309–8321, 2015.
- [33] M. B. Christopher, *Pattern recognition and machine learning*. Springer-Verlag New York, 2016.
- [34] "DJI matrice 200 series v2 specifications," <https://www.dji.com/downloads/products/matrice-200-series-v2>, accessed: 2019.
- [35] BITAG, "Real-time network management of internet congestion," *Broadband Internet Technical Advisory Group*, Oct 2013.